Untargeted metabolomics reveals anion and organ-specific biochemistry of salinity tolerance in willow

Eszter Sas[1], Adrien Frémont[1], Emmanuel Gonzalez[2,3], Mathieu Sarrazin[4], Simon Barnabé[5], Michel Labrecque[1,6], Nicholas James Beresford Brereton[7†] and Frédéric Emmanuel Pitre[1,6]

[1] Institut de recherche en biologie végétale (IRBV), Département de sciences biologiques, Université de Montréal - 4101 Sherbrooke East, Montreal, QC H1X 2B2, Canada
[2] Canadian Centre for Computational Genomics (C3G) - Department of Human Genetics, McGill University, 740 Dr. Penfield avenue, Montreal, QC H3A 0G1, Canada.
[3] Microbiome Research Platform - McGill Interdisciplinary Initiative in Infection and Immunity (MI4), Genome Centre, McGill University, Montreal, QC, Canada
[4] Centre d'Étude des Procédés Chimiques du Québec (CÉPROCQ), Collège de Maisonneuve, 6220 Rue Sherbrooke East, Montréal, QC H1N 1C1, Canada
[5] Département de chimie, biochimie et physique, Université du Québec à Trois- Rivières, 3351 boulevard des Forges, Trois-Rivières, QC G8Z 4M3, Canada
[6] Montreal Botanical Garden, 4101 Sherbrooke East, Montreal, QC H1X 2B2, Canada
[7] UCD School of Biology and Environmental Science, University College Dublin, Belfield, Dublin 4, Ireland

† Corresponding author: nicholas.brereton@ucd.ie

Key words: Salt stress • Metabolomics • *Salix* • Sulfate / Sulfur • Sulphate / Sulphur • Chloride • Anion

1 Abstract

Willows can alleviate soil salinisation while generating sustainable feedstock for biorefinery, yet the metabolomic adaptations underlying their salt tolerance remain poorly understood. Testing two environmentally abundant salts, the response of *Salix miyabeana* was assessed after treatment with a moderate concentration of NaCl, and both moderate and high concentrations of Na_2SO_4 in a 12-week pot trial. Willows tolerated salts across all treatments (up to 9.1dS m^{-1} soil EC_e), maintaining photosynthesis and biomass while selectively partitioning ions, confining Na^+ to roots and accumulating Cl^- and SO_4^{2-} in the canopy, and adapting to osmotic stress via reduced stomatal conductance. Untargeted LC-MS/MS captured over 5,000 putative compounds, characterising the baseline willow metabolome, including 278 core compounds constitutively produced across organs. Comparative statistical analyses revealed widespread metabolic reprogramming in response to soil salinity, altering 28% of the overall metabolome, and highlighting organ-tailored strategies. Comparing both salt forms at equimolar sodium, generalised salinity responses were limited to 3% of the metabolome, predominantly in roots. Anion-specific metabolomic responses were more extensive, with NaCl reducing carbohydrates and TCA intermediates, thereby exerting pressure on carbon and energy resources, alongside the accumulation of root structuring compounds, antioxidants flavonoids, and fatty acids. In contrast, Na_2SO_4 salinity triggered accumulation of sulphur-containing larger peptides, suggesting that excess sulphate incorporation leverage ion toxicity to produce specialized salt-tolerance associated metabolites. This high-depth picture of the willow metabolome underscores the importance of capturing plant adaptations to salt stress at organ-scale and considering ion-specific contributions to soil salinity.

2 Introduction

Soil salinisation represents a major threat to agricultural productivity and environmental health on a global scale. It is estimated that over 20% of irrigated cropland is impacted by salt accumulation (FAO, 2015), reducing yields and biodiversity that is essential for maintenance of functional ecosystems (Hassani et al., 2021; Litalien and Zeeb, 2020; Zörb et al., 2019). Climate change and human activities are predicted to intensify both natural and anthropogenic soil salinisation processes, further threatening food security (Singh, 2021). While research on salt stress typically investigates NaCl due to its prevalence in saline soils, Na_2SO_4, derived from both anthropogenic sources like industrial sulphur emissions and agricultural practices, as well as natural volcanic and marine environments (Dick et al., 2008), represents another widespread salt that can induce species-specific differential susceptibility compared to NaCl (Reginato et al., 2021; Tarchoune et al., 2012). As part of

land management strategies, the use of salt-tolerant biomass crops, which are able to sequester salt in their tissues and improve soil structure and health, could help reclaim and beneficially repurpose salt-impacted areas (Abreu et al., 2022; Quinn et al., 2015).

Soil salinisation results from the accumulation of a variety of soluble ions such as Na^+, K^+, Mg^{2+}, Ca^{2+}, Cl^-, SO_4^{2-} and CO_3^{2-}. When in contact with roots, these ions can induce both osmotic stress and ion toxicity (Munns and Tester, 2008). The osmotic component, primarily driven by any dissolved salt concentration, alters water potential gradients, disrupting cell turgor pressure and elongation. In response, stomatal closure limits water loss via transpiration but also impairs photosynthate supply, ultimately constraining growth through both water deficit and reduced carbon availability (Munns et al., 2020b).

Ion toxicity, however, is dependent on the nature of the ion, with different elements leading to unique patterns of signalling, transport, oxidative damage, energy allocation, and hormone regulated growth processes (Guo et al., 2017; Llanes et al., 2013; Reginato et al., 2021, 2019; Richter et al., 2019). Chloride (Cl^-), an essential micronutrient for plants, contributes to several vital physiological processes (Wege et al., 2017). As a major osmotically active solute, chloride fluxes are involved in vacuolar turgor required for cell expansion and are implicated in the regulation of stomatal aperture, contributing to water balance and gas exchange (Teakle and Tyerman, 2010). Additionally, chloride acts as a counter-ion, regulating membrane potential, intracellular pH gradients, electrical signalling in the cytoplasm (White and Broadley, 2001) and serves as a cofactor in the oxygen-evolving complex of photosystem II (Ifuku, 2015). However, in salt-impacted soils, excess chloride damages plants, leading to impaired photosynthesis, general enzymatic activity (Geilfus, 2018) and reduced NO_3^- uptake (Abdelgadir et al., 2005). In contrast, sulphate (SO_4^{2-}), the major bioavailable form of sulphur, is an essential macronutrient involved in various physiological and biochemical processes (Prasad and Shivay, 2018; Watanabe and Hoefgen, 2019). Sulphur is required for the production of the amino acids cysteine and methionine, peptide derivatives such as glutathione, and disulphide bonds contributing to enzyme activity and stability. The production of chlorophyll, vitamins and certain plant defence specialised metabolites, such as glucosinolates, also depend upon sulphur (Chan et al., 2019; Rausch and Wachter, 2005). Plants regulate sulphate uptake and assimilation through sulphate specific transporters to avoid toxicity (Buchner et al., 2004), however in some crop species such as *Brassica rapa*, excess sulphate ions can create nutrient deficiency by competing with the absorption of other ions, such as calcium and phosphorus (Reich et al. 2017).

Plants mediate salt stress through a coordinated series of physiological, structural, biochemical and molecular adjustments (Arif et al., 2020; Deinlein et al., 2014; Gupta and Huang, 2014; Munns et al., 2020a; Polle and Chen, 2015; van Zelm et al., 2020; Yang and Guo, 2018). Although pathways vary between plant species (Sanchez et al., 2008) and depend on the type of ions involved (Reich et al., 2017; Richter et al., 2019), key tolerance mechanisms include osmotic regulation, ion homeostasis, antioxidant defence, and growth modulation.

A primary adaptive response to osmotic stress is the accumulation of osmolytes, which regulate water status by reducing cell osmotic potential and stabilise proteins and cellular structures (D'Amelia et al., 2018; Yang and Guo, 2018). This response is common to all osmotic stress pathways and is not exclusively induced by excess salt nor is dependent on salt type (Munns, 2002). Osmolytes include inorganic ions (Rodriguez et al., 1997; Wege et al., 2017) and organic compounds such as amino acids (e.g. proline), polyamines (e.g. spermidine), quaternary ammonium compounds (e.g. glycine betaine), sugars (e.g. sucrose, trehalose), and polyols (e.g. mannitol, sorbitol) (D'Amelia et al., 2018; Slama et al., 2015; Yang and Guo, 2018). While the biosynthesis of these osmoprotectants imposes a metabolic energy cost (Munns et al., 2020a), their functions extend beyond osmotic adjustment, serving various detoxification processes, such as antioxidant activity and chaperone-mediated protein stabilisation (Yancey, 2005), as well as potential enzyme regulation. Plants avoid cytotoxicity and maintain ion homoeostasis through salt exclusion from roots, compartmentalisation into the vacuole or apoplast, selective transport and excretion through salt glands. The upregulation of enzymatic (e.g. superoxide dismutase SOD, catalase CAT, peroxidase POX) and non-enzymatic (e.g. glutathione, ascorbate, flavonoids, anthocyanins) antioxidants is crucial for mitigating damage to cellular components such as lipids, proteins, and DNA caused by reactive oxygen species (ROS) (Gill and Tuteja, 2010a). Additionally, hormonal signalling (Ryu and Cho, 2015), salt avoidance via modification of root architecture (Zou et al., 2022), xylem alteration and loading (Janz et al., 2012) and symbiotic associations with microorganisms such as arbuscular mycorrhizal fungi (Evelin et al., 2009) also play significant roles in enhancing plant tolerance to salinity.

Salicaceae, including poplars (*Populus sp.)* and willows (*Salix sp.*), are common phytoremediation and biorefinery crops on marginal lands (Brereton et al., 2017; Dimitriou and Aronsson, 2005; Gonzalez et al., 2018; Rodzkin and Volk, 2018; Sas et al., 2021; Volk et al., 2006), with high potential for growth on salinised soils. For example, some cultivars can maintain transpiration and growth under saline conditions up to 6-8 dS m^{-1} (Bilek et al., 2020; Chen and Polle, 2010; Huang et al., 2020; Jerbi et al., 2020; Mirck and Zalesny, 2015, 2015; Steppuhn et al., 2008). In willows, this tolerance likely engages high metabolic diversity, including reactive oxygen species (ROS) protective phenolics and other antioxidants (Sui and Wang, 2020; Zhou et al., 2020). However, understanding of the metabolomic toolkit employed beyond these target compounds remains limited, particularly concerning its variation across different organs and salts.

In this study, the shared and unique metabolomic adjustments to moderate NaCl, moderate Na_2SO_4 and high Na_2SO_4 salinity treatment were assessed across multiple organs (Fig.1) to determine generalised and ion-specific salt tolerance metabolome in willow.

3 Methods

3.1 Experimental design, plant growth, sample collection and physiological traits

The willow cultivar *Salix miyabeana* 'SX64' was grown from cuttings in a polyethylene grow tunnel within 15 L pots filled with all-purpose growing soil (Promix^{TM}), sand and vermiculite (1:1:1 volume-based). After 56 days of growth for root establishment, salt treatments were applied every 3 days during watering over 28 days to progressively build up soil salinity and to avoid salt shock response (Shavrukov, 2013). The four treatments were: tap water control (EC_{water}=0.3 mS cm^{-1}), 51mM NaCl ($EC_{solution}$=6.5 dS m^{-1}) and 26mM Na_2SO_4 ($EC_{solution}$=6.7 dS m^{-1}), both considered moderately saline, and 51mM Na_2SO_4 ($EC_{solution}$=13.4 dS m^{-1}), considered highly saline (Mirck and Zalesny, 2015). The treatments were arranged in a randomised block design with seven replicate plants (seven independent pots, n=7) per treatment (Fig.1). Leaves, stems, and roots were sampled after 28 days of treatment (84 days of growth). A representative subsample of each fraction was immediately flash-frozen in liquid nitrogen and stored at -70°C for metabolomic analysis.

Shoot heights and numbers were measured weekly. Fresh weight (FW) at harvest, oven-dried biomass weight (DW) and moisture content were measured for each organ. The LICOR-600 porometer/fluorometer was used to measure photosynthetic parameters, including stomatal conductance and the quantum efficiency in light of photosystem II ΦPSII (Genty et al., 1989). Soil salinity was inferred at harvest from electroconductivity of the supernatant solution from a soil:water mixture (1:1) and converted to the electroconductivity of saturated soil extract (EC_e) using the correlation EC_e=2.23 $EC_{(1:1)}$-0.58 (R^2=0.98) established by Sonmez et al. (2008) for combined soil texture.

Elemental analysis of roots, stems, and leaves were performed on ground dry biomass (<500 µm) by Natural Resources Analytical Laboratory at University of Alberta (AB, Canada). Briefly, 0.1±0.02 g of sample was digested overnight, with 5 mL of Trace Metal Grade HNO_3 using the Microwave Accelerated Reaction System (method EPA 3051a (modified)), diluted to 25 mL with milliQ water and analysed for mineral nutrients (Al, B, Ca, Cu, Fe, K, Mg, Mn, Mo, Na, Ni, P, S, Zn) using a Thermo iCAP6300 Duo inductively coupled plasma-optical emission spectrometer (ICP-OES). The anions Cl^- and SO_4^{2-} were determined by extracting 0.2±0.01 g of dry sample with 50 mL of 2% acetic acid using a reciprocal shaker for 30 min, followed by a 0.45 µm PTFE syringe filtration. Chloride and sulphate were measured using the ferrithiocyante colorimetric method (EPA Method 325.2) and the barium chloride turbidimetric method (EPA Method 375.4), respectively.

3.2 Extraction of metabolites

Metabolites from willow roots, stems and leaves were extracted according to De Vos et al. (2007) with some modifications. Briefly, plant tissues were freeze-dried for 72 hours and homogenised using a precooled bead mill Tissuelyser II (Qiagen) at 30 Hz, for 2-4 cycles of 60 seconds each. From the dry tissue powder, 50±0.5 mg was suspended in 1 mL of methanol:water (75:25%v/v), also containing the internal quantitative standard resorcinol at 5 mmol L^{-1}. Samples were vortexed for 10 s, sonicated in a 135 W/42 Hz ultrasound bath for 10 min at room temperature and centrifuged at 11,000xg for 2 min at 20°C. The supernatant was filtered through a 0.2 µm centrifuge filter, diluted by 4 with methanol 75% and placed in the LC-MS/MS autosampler conditioned at 4°C.

3.3 Liquid chromatography-tandem mass spectrometry (LC-MS/MS) acquisition

Chromatographic separation was performed using an Agilent 1260 Infinity system, where 10 µL of extract was injected onto a Zorbax Eclipse Plus C18 column (4.6 × 100 mm, 3.5 µm) at 30 °C. Mobile phase was solvent A (water, 5% methanol, 0.1% formic acid) and solvent B (methanol, 0.1% formic acid) with a flow rate of 0.4 mL min^{-1} and an 80-minute elution gradient: 100% A hold for 20 min, then a linear increase from 0% to 100% B over 50 min and 100% B hold for 10 min. This gradient allowed detection of highly water-soluble (polar) compounds within the first isocratic phase. Untargeted full-scan (100–1,300 Da) MS acquisition was performed on extracts from all three organs (roots, stems and leaves) of each of the seven replicates (84 samples total), blanks and quality control samples using an Agilent Q-TOF 6530B mass spectrometer equipped with an Agilent Jet Stream ion source operating in positive ion mode (ESI (+)). Gas temperature was 300 °C, drying gas flow was 5 L min^{-1}, and the nebuliser pressure was 45 psig. Sheath gas temperature was 250 °C with a gas flow of 11 L min^{-1}. Data-dependent MS/MS acquisition was performed on three biological organ replicates per treatment and acquired at collision energy of 20 and 35 eV. Precursor isolation used an intensity threshold set to 500, with a maximum of 4 precursors per cycle and 3 spectra per precursor released after 0.3 min.

3.4 Untargeted metabolite data processing

Raw LC-MS data were converted to mzML files by using msConvert (Chambers et al., 2012) and processed using MZmine 3.3.0 (Schmid et al., 2023) (Fig.1). Background noise cut-off was 1,000 for MS spectra and 0 for MS/MS spectra, with a minimum 3,000 peak intensity threshold for feature detection. Chromatogram deconvolution used the local minimum search algorithm, isotopes were grouped and features alignment across samples was performed with 20 ppm mass tolerance (80% weighting) and 1 min retention time tolerance (20% weighting). Feature quality control filtering applied isotope patterns (minimum two), minimal occurrence of four across all samples, and a maximal blank:sample average ratio (1:3). Features eluting within <0.2 min retention time and with peak shape correlated by >85% (MZmine metaCorrelate algorithm) were assigned to a feature correlation group and used for curation of adducts, complex formation, and in source fragments.

3.5 Metabolites annotation and molecular networking

The feature annotation pipeline used unsupervised and supervised searches across multiple databases integrated with cheminformatic tools (Fig.1). An initial unsupervised annotation step used *in silico* prediction with SIRIUS, combining raw formula and structural elucidation CSI:FingerID (Dührkop et al., 2019), as well as compound class annotation with CANOPUS (Dührkop et al., 2020). In parallel, all features were searched against a set of MS and MS/MS databases, including general databases available in the GNPS environment (including GNPS, MassBank and ReSpect) as well as experiment- and organism-specific databases (PlantCyc (Hawkins et al., 2021), CEU mass mediator (Gil-de-la-Fuente et al., 2019), an in-house library for Salicaceae based on literature as well as authentic standards). Annotation candidate information was standardised for comparison across tools, and the best hit for each feature selected after quality assessment and prioritisation based on integrated confidence/accuracy scores, MS/MS alignment scores, and MS match precision (minimal difference between experimental and predicted compound mass, adduct prediction) to generate a list of putative compounds from combined tools outputs.

In a second supervised step, annotation of significantly differentially abundant compounds was refined using data-driven and knowledge-based curation. Data-driven curation uses feature-based ion identity molecular networking (Z. Zhou et al., 2022) based on cosine and/or Spec2Vec metrics (Huber et al., 2021) of spectral similarity within subnetworks, and manual resolution of ambiguities. Knowledge-driven curation takes advantage of published compound lists and spectra from comparable experiments and plant species not deposited in public databases to improve annotation.

Each putative compound annotation is assigned a confidence level (1-4) (Schymanski et al., 2014; Sumner et al., 2007) and is reported in supplementary data tables, following best reporting practices (Alseekh et al., 2021). Chemical taxonomy was assigned to metabolites using the Natural Product Classification system (Kim et al., 2021). Molecular networks were generated in the GNPS analysis environment (Nothias et al., 2020) and visualisation used cosine metrics (at 0.6 threshold) within Cytoscape software (Shannon et al., 2003).

3.6 Statistical analysis

Physiological and metabolomic data were processed using R (R Core Team, 2022) and statistical significance was set at a Benjamin-Hochberg (BH) false discovery rate (FDR) adjusted p-value threshold of <0.05. Physiological comparisons between treatments used a two-way ANOVA, followed by a Tukey HSD *post hoc* test

(n=7, except n = 3 for mineral element analysis). Metabolite peak areas were log-transformed and normalised using EigenMS (Karpievitch et al., 2014) prior to statistical analysis (Fig.1). To identify differentially abundant (DA) metabolites, pairwise comparisons of peak area for each treatment (n=7) were performed against controls using either a t-test or Wilcoxon rank sum test with FDR (BH) control, depending on whether assumptions of normality and equal variance were met, or through detection as structural zeros (He et al., 2014) (metabolites detected ≥4 replicates of one condition, and not detected in any replicates of the compared condition). For metabolite comparison across organs, a Kruskal-Wallis test was first performed before *post hoc* pairwise comparisons between each organ pair (Wilcoxon rank sum tests with FDR control). The core metabolome was tentatively defined as compounds that did not significantly vary across control organs and meet a metabolic stability coefficient of variation of peak area below 30%. Principal component analysis (PCA) was performed using MixOmics package (Rohart et al., 2017) and PERMANOVA on Bray-Curtis distances was used to test significant differences between groups.

4 Results

4.1 Physiological effects of salt treatments and mineral elements accumulation

After 28 days of salinity treatments, soil electrical conductivity (EC_e) was 0.9±0.2 dS m^{-1} in controls (Fig.2a) and was significantly higher in both moderate NaCl and Na_2SO_4 treatments, at 6.5±0.2 and 5.5±0.5 dS m^{-1} (Tukey HSD, $\alpha<0.05$). High Na_2SO_4 significantly increased soil conductivity further to 9.1±0.5 dS m^{-1}.

Willows maintained a healthy phenotype throughout the experiment (Fig.2b) and salt treatments did not induce significant differences in aboveground growth rate nor in leaf, stem, or root biomass yields when compared to controls (Supplementary – Fig.S1-S3), with an average total biomass of 131±5 g dry matter (DM) (Fig.2c). Quantum efficiency ΦPSII ranged from 0.44-0.61 and was not significantly different between control and salt-treated willows (Fig.2d). Salt-treated willows showed significant reductions in stomatal conductance to water vapor (g_{sw}) ranging from 0.13-0.19 mol m^{-2} s^{-1} (Fig.2e), compared to g_{sw} of 0.29±0.04 mol m^{-2} s^{-1} in control willows. Leaf moisture content (MC) was 1.97±0.07 g_{H2O} g_{DM}^{-1} in controls and significantly increased to 2.28±0.10 g_{H2O} g_{DM}^{-1} under moderate NaCl treatment. Moderate Na_2SO_4 resulted in intermediate leaf MC, at 2.09±0.04 g_{H2O} g_{DM}^{-1}, while high Na_2SO_4 treatment significantly decreased compared to both moderate salt treatments, measuring 1.75±0.04 g_{H2O} g_{DM}^{-1} (Fig.2f). None of the treatments induced significant differences in stem moisture content, which was maintained at an average of 1.34±0.03 g_{H2O} g_{DM}^{-1}.

The elemental analysis indicated salt treatments increased the salt ion contents (Fig.3a). Specifically, the total content of sodium was 2.78±0.1 mmol(Na) in controls, 9.4±0.3 mmol(Na) in moderate NaCl, 10.1±0.1 in moderate Na_2SO_4 and 13.0±0.1 mmol(Na) in high Na_2SO_4-treated willows. Comparison of concentrations at the organ scale (Fig.3b) revealed that the sodium concentration is highest in roots and increased 3-fold compared to controls, regardless of the salt treatment. Total chloride content was significantly higher in NaCl treatment, with 26.3±2.1 mmol(Cl) as compared to an average of 6.8±0.2 mmol(Cl) for controls and Na_2SO_4 treatments. In NaCl treatment, leaves had the highest concentration of Cl at 575.4±26.5 µmol(Cl) g_{DW}^{-1}, representing a 3.4-fold increase compared to controls; while accumulation in stems and roots was below 190 µmol(Cl) g_{DW}^{-1}, but still resulting in a 4.3 to 5.5-fold increase compared to controls. Total sulphur content was significantly higher in both Na_2SO_4 treatments, at similar 14.1±0.5 and 15.7±1.9 mmol(S), as compared to 7.4±0.4 mmol(S) in controls and 8.5±0.2 mmol(S) in NaCl. Sulphur concentration significantly increased in concentration from 84.3±6.1 µmol(S) g_{DW}^{-1} in control roots to an average of 147.9±6.1 µmol(S) g_{DW}^{-1} in Na_2SO_4-treated roots and from 161.0±11.1 µmol(S) g_{DW}^{-1} to 229.1±7.5 µmol(S) g_{DW}^{-1} in leaves. At the whole plant scale, the proportion of inorganic sulphur did not vary significantly across treatments, averaging 27% of the total sulphur present as inorganic SO_4^{2-} (Supplementary – Fig.S5). Total potassium content was 21.3±0.6 mmol(K) in controls and significantly higher in both moderate and high Na_2SO_4 treatments, with similar content of 28.9±0.2 and 28.4±2.3 mmol(K) respectively. Potassium concentration tended to decrease in salt-treated roots but increase in salt-treated leaves compared to controls. Conversely, phosphorus concentration tended to increase in salt-treated roots while decreasing in leaves; however there was no significant variation across all four treatments in total phosphorus, measured at an average of 5.4±0.4 mmol(P). Across all four treatments, there were no significant variations in total calcium and magnesium content, averaging 29.3±0.5 mmol (Ca) and 6.9±0.6 mmol(Mg). However, calcium concentration in leaves significantly decreased in both Na_2SO_4-treated plants compared to controls while leaf magnesium concentration significantly increased in NaCl-treated plants only, compared to controls.

4.2 Organ partitioning of the Salix metabolome

After 84 days of growth, untargeted metabolomic profiling of control willows, without salt treatment, revealed a total of 5,043 metabolic compounds across all three organs, with 2,063 compounds in roots, 2,950 compounds in stems, and 3,601 compounds in leaves (Fig.4a). Shannon and inverse Simpson indices showed a significant sequential increase in metabolic diversity from roots to stems to leaves (Fig.4b). Principal Component Analysis (PCA) separated samples based on organ (Fig.4c), PC1 and PC2 explaining 52% and 26% of variance, respectively, with significant differences between groups (*PERMANOVA*, p-value<0.05). Leaves and stems exclusively shared 481 compounds, stems and roots exclusively shared 371 compounds while leaves and roots exclusively shared 83 compounds (Fig.4d).

A total of 1318 compounds were present in all three organs (Fig.4d), representing 73-96% of cumulative peak area in each organ (approximate of abundance; Fig.4e). Differential abundance comparison between organs showed that, of these shared compounds, 278 did not significantly differ. They were defined as "core metabolites" and included 29 flavonoids, 14 phenolic acids, 12 phenylpropanoids, 22 small peptides, 11 tryptophan alkaloids, 9 pseudoalkaloids, 10 nucleosides, 8 saccharides, 8 monoterpenoids and 4 fatty acids and conjugates (Fig.4f). Some high-intensity compounds were adenosine, glutamate, 12-tetradecenoic acid, myrciacitrin III, apigenin 7-O-neohesperidoside, kaempferol 3-O-glucoside (astragalin), salicortin, salicin, benzaldehyde, 4-o-caffeoylshikimic acid, secoxyloganin, 7-O-p-coumaroyl loganin, nicotinamide, galactosylglycerol and fructose (Supplementary data tables).

Conversely, 3,259 compounds were defined as organ-specialised metabolites as they had significantly higher abundance in one organ compared to the other two, including 1,719 compounds exclusively detected in leaves, 780 in stems and 291 in roots. Leaf-specialised compounds were dominated by the terpenoid pathway (Fig.4g), with a high number of (seco)iridoid monoterpenoids, diterpenoids, steroids, (apo)carotenoids, as well as the alkaloids pathway, particularly tyrosine and tryptophan derived alkaloids. Stem-specialised compounds were dominated by phenylpropanoids, lignans and fatty esters whereas root-specialised compounds were dominated by saccharides and amino acids glycosides. Each organ also had a highly specific set of flavonoids and small peptides. Interestingly, 19% of root-specialised compounds were highly water soluble (polar), compared to 5% of stem-specialised and 10% of leaf-specialised compounds (Supplementary – Fig.S6).

4.3 Salix metabolomic response to moderate and high Na_2SO_4

When comparing metabolomic differences under various Na_2SO_4 concentrations, PCA separated samples by control, moderate and high Na_2SO_4 treatments in roots *(PERMANOVA*, p-value<0.05), with PC1 explaining 17% and PC2 explaining 11% of the variance, while no separation was observed between treatments in stems and leaves (Fig.5a). Moderate Na_2SO_4 led to 571 DA compounds across the whole plant, including 218 in roots, 105 in stems and 248 in leaves (Fig.5b,d). Comparatively, high Na_2SO_4 led to 976 DA compounds across the whole plant, including 574 in roots, 131 in stems and 271 in leaves (Fig.5c,d).

Taken together, the Na_2SO_4-salt response involved 989 compounds distributed across the main pathways as 260 shikimates/phenylpropanoids, 133 alkaloids, 84 carbohydrates, 79 amino acids/peptides, 73 terpenoids, 51 fatty acids and 25 polyketides (Fig.5e). In response to moderate Na_2SO_4 treatment, significant deplition represented 58-60% of the changes in roots and stems, while enrichment represented 85% of changes in leaves (Fig.5d,h). Higher Na_2SO_4 induced a larger metabolite enrichment across most pathways, except for further depletion in carbohydrates, while stems maintained a reduced metabolite pattern and leaves maintained increased metabolites across the major pathways.

Over the whole plant, 327 compounds were consistently DA in both moderate and high Na_2SO_4 treatments, representing 21% of DA compounds in roots, 24% in stems and 53% in leaves (Fig.5f). This consistent response was further reflected in a R^2=0.93 correlation between the fold changes (log_2) of control *vs* moderate Na_2SO_4 and control *vs* high Na_2SO_4 treatments (Fig.5g).

In roots, moderate Na_2SO_4 reduced 45 compounds within shikimates/phenylpropanoids pathway, including 15 flavonoids, 9 phenolic acids and 5 lignans (Fig.5h). Comparatively, high Na_2SO_4 treatment increased 113 compounds from that pathway, including 52 flavonoids, 12 phenolic acids, 12 phenylpropanoids as well as 10 lignans. These included enrichment of important compounds such as 4-coumaroyl shikimate, 5-hydroxyferulate, procyanidol, catechin 3-O-(1-hydroxy-6-oxo-2-cyclohexene-1-carboxylate), 8-hydroxypinoresinol 4'-glucoside, guaicylglycerol-coniferyl ether, glucose-conjugated salicylic acid, and salicin. Six sphingolipids, including phytosphingosine and 4-hydroxysphinganine, were consistently depleted by both

Na_2SO_4 concentrations, while 4 and 10 saccharides significantly reduced under moderate and high Na_2SO_4, respectively. In contrast, 8 nucleosides and 20 small peptides increased only under high Na_2SO_4, as did 8 pseudoalkaloids, 8 tryptophan alkaloids, 6 tyrosine alkaloids, 12 monoterpenoids, 11 steroids and 9 triterpenoids. In stems, moderate and high Na_2SO_4 treatments enriched 3 and 7 small peptides, such as aspartate and proline, while 7 and 8 small peptides were depleted, respectively. Additionally, 4 and 14 saccharides were depleted, including glucose and trehalose (Fig.5h), whereas 14 and 13 saccharides were enriched in leaves. Furthermore, common, dose-responsive compounds in leaves were dominated by 49 shikimates/phenylpropanoids, encompassing enrichment of 9 cinnamic acid derivatives, 5 salicinoids and 4 other simple phenolic acids, 4 flavonols and 4 chalcons. Commonly regulated metabolites also included 25 alkaloids and 20 amino acids/peptides, with the enrichment of 7 pseudoalkaloids (5 purine and 2 pteridine alkaloids), 3 tryptophan alkaloids and 15 small peptides (Fig.5h).

A total of 179 DA responses to one or both concentrations of Na_2SO_4 (12% of all Na_2SO_4 metabolomic changes) contained sulphur, corresponding to 101 distinct compounds. Roots significantly accumulated 13 and 45 sulphur compounds (S-compounds) under moderate and high Na_2SO_4 respectively, but significantly reduced 4 and 20 S-compounds (Fig.5i). Additionally in leaves, 36 compounds were increased under one or both Na_2SO_4 concentrations, compared to 11 depleted S-compounds. Shared enriched S-compounds included dicarboxylic acid such as 2-(2-sulfoethyl)propanedioic acid or polyamines, such as N'-hydroxy-5-(2-methoxyethyl-sulfamoylamino) pentanimidamide, as well as stilbenes, such as resveratrol 4-sulfate. High Na_2SO_4 depleted S-containing compounds ranged from small peptides, such as threonine to larger alkaloids such as $C_{19}H_{16}N_8O_5S$ (CHEMBL164867). Notably, a subgroup of 16 DA S-compounds were in the same structural cluster (Fig.5j).

4.4 Salix metabolomic response to NaCl treatment

Comparing controls with NaCl-treated willows, principal component analysis of root, stem, and leaf metabolites revealed a significant separation between control and NaCl treatment in roots (*PERMANOVA*, p-value<0.05), partial overlap in stems (*PERMANOVA*, p-value<0.05) and no observed separation in leaves (Fig.6a). NaCl treatment led to 1,063 DA responses compared to control trees, with 475 DA compounds in roots, 481 in stems and 107 in leaves (Fig.6b). Among these, 768 responses were unique to one organ, while 135 DA compounds were shared to two or all organs (Fig.6c). Notably, 98 compounds were exclusively shared between roots and stems and 24 compounds were significantly depleted in all three organs due to NaCl treatment.

Across all organs, NaCl-responsive metabolites comprised 213 DA compounds within the shikimates/phenylpropanoids pathway, 118 alkaloids, 88 carbohydrates, 74 amino acids/peptides, 59 terpenoids, 48 fatty acids and 12 polyketides (Fig.6d). While shikimates/phenylpropanoid pathway compounds were the most diverse in responding to NaCl, carbohydrates represented the highest proportional change within a pathway, constituting >33% of total carbohydrates (Supplementary – Fig.S7). This was driven by significant depletion in 28 carbohydrates across multiple organs, including glucose, fructose, sucrose and valienol 1,7-diphosphate, as well as organ-specific depletion of 36 carbohydrates (Fig.6e,f). Tricarboxylic acid cycle intermediates, such as malate, citrate, 2-oxoglutarate, and phosphorylated compounds, such as phosphocholine, phosphonoacetaldehyde, 1,7-diphospho-1-epi-valienol and 2-C-methyl-D-erythritol-2,4-cyclodiphosphate, were other examples of depleted compounds across the entire plant (Supplementary – Fig.S8).

Within organs, leaves had a limited response to NaCl treatment (Fig.6b,c), but depleted compounds included 2-oxoglutarate, malate, aspartate and choline, while accumulated compounds included populoside C, (indol-3-yl)acetyl-myo-inositol L-arabinoside (IAA derivative) and spermidine (Supplementary data tables – **Error! Reference source not found.**). Stems and roots had a larger metabolic response, markedly within the shikimate/phenylpropanoid pathway, altering 115 and 108 compounds respectively (Fig.6e). This large group of differentially abundant phenolic compounds was primarily associated to flavonoids, phenylpropanoids, lignans and phenolic acids (including salicinoids). While flavonoids were similarly enriched in stems (20 DA compounds) and roots (23), this phenolic superclass was substantially more depleted in stems (23) than in roots (10) (Fig.6h). Salicinoids had a net enrichement in both stems and roots (Fig.6h). Stem metabolomic responses featured the significant accumulation of myricetin 3-O-glucoside, kaempferide 3-O-glucoside, procyanidol, salicin and grandidentatin, alongside the depletion of eriodictyol 7-glucuronide, luteolin 7-(6''-benzoylglucoside, ramontoside and a hydroxycyclohexen-oyl ester catechin derivative. In roots, (iso-)salicin, salicylic acid glucoside, grandidentatin, catechin, procyandin C, pleurostimin 7-glucoside were depleted, and populin, tremuloidin and benzoyl-β-D-glucoside were enriched. Additionally, 21 lignans and phenylpropanoids

accumulated in roots, contrasting stems, where 14 lignans and phenylpropanoids were significantly depleted (Fig.6h).

A balanced pattern of metabolomic change was observed in nitrogen metabolism in response to NaCl treatment, with enrichment of 147 DA compounds and depletion of 133 DA compounds. This was particularly evident as 31 small peptides increased across all organs, including proline, tryptophan and glutathione, while 34 small peptides decreased, including acetylproline, threonine and arogenate (Fig.6g). Other increasing N-containing compounds included purine nucleosides like adenosine, alkaloids such as dihydrosanguinarine and kinetin-7-N-glucoside, as well as sphingolipids, such as phytosphingosine and sphinganine. Concurrently, the response to NaCl treatment significantly increased terpenoids, especially monoterpenoids, with 15 enriched monoterpenoids in stems and 13 in roots (Fig.6i,j).

4.5 Salix anion-specific metabolomics response to NaCl and Na_2SO_4 (at the same EC)

Comparing the 1,063 and 571 DA compounds altered by moderate NaCl and moderate Na_2SO_4 revealed 103 DA compounds commonly regulated in roots, 53 in stems and 7 in leaves (Fig.7a,b). These generalised salinity responsive metabolites included 23 shikimates/phenylpropanoids, 10 alkaloids, 10 carbohydrates, 9 terpenoids, 9 amino acids and peptides and 5 fatty acids (11 other and 70 unknown) (Fig.7b). Commonly enriched compounds included (indol-3-yl)acetyl-myo-inositol L-arabinoside and 2-phenylacetamide in leaves; proline, grandidentatin and fraxiresinol 1-O-glucoside (a lignan) in stems; 2-thioethylidenebis(phosphonic acid), delphinidin 3-O-(6''-O-malonyl)-beta-D-glucoside-3',5'-di-O-beta-D-glucosideand and syringin in roots. Commonly depleted compounds included glucose, trehalose in stems; D-altro-heptulose, glycerophophoglycerol, benzoyl-beta-D-glucoside and N-(4-(1-Cyanocyclopentyl)phenyl)-2-((pyridin-4-ylmethyl)amino)nicotinamide in roots; as well as d-glycero-l-galacto-octulose in both stems and roots.

Distinct from generalised response, 764 DA compounds were unique to moderate NaCl treatment, while 391 DA compounds were unique to the moderate Na_2SO_4. The DA compounds unique to NaCl included a net reduction of 29 saccharides, 16 nucleosides and 6 aminosugars. The DA compounds unique to moderate Na_2SO_4 treatment included a net accumulation of 19 small peptides, 10 nucleosides, and 10 saccharides (Fig.7c).

An anion-specific effect could be observed when comparing the response of constitutively produced compounds that were core (present and relatively stable between organs) and organ-specialised (significantly different between organs), but also in salt-induced compounds (not detected in controls). In both moderate salt treatments, roots primarily reduced organ-specialised compounds rather than core compounds, while significantly enriched compounds were predominantly salt-induced rather than root-specialised or core compounds (Fig.7d). Similarly, in stems, reduced compounds were largely organ-specialised rather than core compounds under both salt types, however enriched compounds were predominantly stem-specialised under NaCl, with 53 enriched compounds as compared to 20 salt-induced and 23 enriched core compounds. Conversely, Na_2SO_4 treatment resulted in 5 salt-induced, 3 enriched core, and 2 enriched stem-specialised compounds. Finally, in leaves, NaCl treatment reduced 13 organ-specialised and 4 core compounds while elevating 26 leaf-specialised and 4 core compounds, as well as inducing 20 new compounds. In contrast, leaves treated with Na_2SO_4 largely decreased leaf-specialised compounds while broadly increasing core compounds.

5 Discussion

5.1 Salix salinity tolerance response

Soil salinity levels are commonly categorised based on EC_e as slightly saline (2-4 dS m^{-1}), moderately saline (4-8 dS m^{-1}), and highly saline (>8 dS m^{-1}) (Corwin and Scudiero, 2019; FAO, 1988). Here, the comparison of non-saline control, moderately saline NaCl and Na_2SO_4, and highly saline Na_2SO_4 (Fig.2a) enabled to capture the anion-specific effects (Cl^- and SO_4^{2-}) and severity effects (moderate vs high Na_2SO_4) on willow (*Salix miyabeana* 'SX64').

Salix miyabeana photosynthetic capacity and biomass productivity were maintained compared to water controls, even at high soil salinity levels of 9 dS m^{-1} (Fig.2c,d), supporting suitability of willow for phytoremediation. This aligns with research by Hangs et al. (2011), reporting salinity tolerance in 37 willow varieties, where most cultivars could tolerate moderate soil salinity (5 dS m^{-1} EC_e) and the most salt-tolerant cultivars maintained biomass productivity even under high soil salinity (8 dS m^{-1} EC_e).

A salt effect was observed on leaf moisture content, which increased under moderate salinity, alongside a >35% reduction of stomatal conductance (Fig.2e). This indicates reduced transpiration accompanied by osmotic adjustment to sustain turgor, potentially mitigating ion toxicity through absorbed salt dilution (Munns et al., 2020b; Nguyen et al., 2017). However, subsequent lower leaf moisture content suggests this water balance might not be maintained as salinity severity increase (Fig.2d).

Salt treatments did not impede the acquisition of essential nutrients and even stimulated potassium uptake alongside salt ions, although willow demonstrated selective partitioning of these ions (Fig.3). Sodium accumulation by the plant was predominantly restricted to the roots and its influx did not exhibit a linear increase in relation to the external concentration, suggesting a robust sodium exclusion mechanism (Fig.3a). Such exclusion can occur through the binding of Na^+ to root cell wall component (Byrt et al., 2018) or a competing uptake of K^+ (Hauser and Horie, 2010), as proposed in the salt tolerant *Salix interior* (Major et al., 2017) and *Salix eriocephala* 'LAR' (Huang et al., 2023). In contrast, the high chloride uptake and transport throughout the plant (Fig.3) may have been facilitated by passive anion channels (Skerrett and Tyerman, 1994), resulting in leaf chloride concentrations here reaching the upper optimal level for non-halophytes, estimated to range from 30 to 560 µmol(Cl) g_{DW}^{-1} (Geilfus, 2018). This accumulation, coupled with increased leaf water content, suggests that Cl^- may serve as a readily available osmolyte, potentially conferring osmotic benefits similar to those observed in *Nicotiana tabacum* (Franco-Navarro et al., 2016). However, given that cytosolic chloride toxicity is thought to occur at concentrations of 5-20 mmol(Cl) L(cytosol)$^{-1}$ (Teakle and Tyerman, 2010), the accumulated Cl^- may also require compartmentalisation into vacuoles, apoplasts, or older leaves to mitigate cellular damage and optimise metabolic burden. In comparison to chloride, sulphate uptake was more constrained but still resulted in increased transport throughout the entire plant, where it was either stored as SO_4^{2-} or metabolised into organic sulphur compounds.

The maintenance of biomass yields despite reduced stomatal conductance, which can lead to decreased carbon assimilation (Munns et al., 2020a), suggests effective metabolic plasticity and ion management strategies, making this experimental system suitable for assessing willow metabolomic tolerance mechanisms without the confounding metabolic effects associated with severe salt-induced physiological damage.

5.2 High organ-specific diversity in the Salix metabolome

Untargeted metabolomic analysis of control trees revealed substantial diversity across the three main vegetative organs (roots, stems and leaves), with over 5,000 compounds detected, approximately 62% of which could be annotated at confidence levels 1-3 (Sumner et al., 2007), providing a comprehensive overview of the willow metabolome at whole plant scale (Fig.4). Previous metabolomic studies in single organs of *Salix* have captured up to 1,639 metabolites in bark (J. Zhou et al., 2022), 2,735 (Kaling et al., 2015), 600 (Jia et al., 2020) and 2,440 (Aliferis et al., 2015) metabolites in leaves, and 800 metabolites in roots (Xia et al., 2021). By integrating all major organs in the analysis, a group of common metabolites across organs were identified, representing 26% of metabolomic diversity and over 70% of the putative abundance (estimated from peak area) (Fig.4d). Of these, 287 metabolites had stable abundance across organs and represent its potential plant-wide basal, or "core", metabolism (Fig.4f); a recent metabolomic concept that can also denote evolutionarily conserved metabolites across species (Drapal et al., 2022; Dussarrat et al., 2022; McLaughlin et al., 2023). Many of these core metabolites were associated with central pathways like glycolysis, TCA cycle derivatives, and amino acid metabolism, reflecting primary metabolism across plant tissues. Others, such as shikimates/phenylpropanoids, align with high levels of bioactive phenolics found in Salicaceae, especially the characteristic salicylates (e.g. salicin, salicortin), associated to antioxidant, antimicrobial and anti-herbivory functions in willow (Boeckler et al., 2011; Brereton et al., 2017; Meier et al., 1988; Pobłocka-Olech et al., 2007; Tyśkiewicz et al., 2019; Volf et al., 2015).

Beyond these commonalities, willow organs had clear metabolic differences (Fig.4g). Leaves contained the most diverse metabolome, aligning with leaf function as a source of complex photosynthates. The leaf metabolome included diverse terpenoids involved in light harvesting, development, defence, and signalling (Pichersky and Raguso, 2018). Stems accumulated lignans, and phenylpropanoids, reflecting the role of this woody tissue in structure and storage (Boeckler et al., 2011; Köhler et al., 2020). Additionally, the metabolic profile of stems had a larger overlap with those of leaves and roots, underscoring their function as metabolic conduits for transport and dialog between aerial and belowground processes (Fig.4d). Comparatively, despite critical functions of water and nutrient absorption, exudation, anchoring structure and storage, roots had the lowest metabolic diversity (Fig.4a,b). Roots were enriched in saccharides and flavonoids, thought to mediate

soil interactions like microbial symbiosis (Endo et al., 2021), metal tolerance (Osawa et al., 2011), and nutrient uptake (Cesco et al., 2012) as well as play a possible role in root architecture, either directly or indirectly (for example through auxin modulation), influencing processes such as gravitropism, root elongation, lateral root and root hair development (Buer et al., 2010). The root metabolome was also distinctly richer in polar metabolites (Supplementary – Fig.S6) which can more readily diffuse through the soil environment within the water vector and could therefore play a role as exudates involved in shaping the rhizospheric biotic (Sasse et al., 2018) and abiotic (Badri and Vivanco, 2009) environment.

These distinct metabolomes reflect the different physiological roles of each organ, describing different metabolic activity and degree of functional specialisation (Li et al., 2016) as well as serving as a baseline to enable understanding of key responses to stimuli such as salt stress.

5.3 Sulphate salt induce dose-dependent metabolomic responses in Salix

Sulphate salinity induced extensive organ-specific metabolic reprogramming (Fig.5a-d,h), affecting 10% and 16% of all metabolites at moderate and high concentrations, respectively. Doubling the Na_2SO_4 concentration in soil from moderate to high levels resulted in a twofold increase of metabolic changes in roots, whereas the range of responses in stems and leaves remained limited. This localisation of metabolic response to the roots, which serve as the primary barrier of defence against excess ions and osmotic stress, is likely decisive in mitigating salinity stress impacts on aerial parts. Notably, consistent levels of salt ion uptake and accumulation despite increased soil salinity indicate effective ion management (Fig.3), allowing leaves to maintain similar adaptative metabolomic strategies under both sulphate salt treatments (Fig.5f,g). Previous studies reported sulphate salt tolerance in willows (Huang et al., 2020) associated with ion imbalance restriction to roots, similarly preventing physiological impacts on leaves at salinity levels up to 7 dS m^{-1} (comparable to moderate Na_2SO_4).

In roots, Na_2SO_4 dose had a differential effect on shikimates/phenylpropanoids, with a reduction of flavonoids, phenolic acids and lignans under moderate level, contrasting their net increase under higher sulphate salinity (Fig.5h). This may indicate a developmental slowdown under mild stress, superseded by a required metabolic burst under more severe salinity levels. The lower osmotic potential associated with higher salinity likely drove the accumulation of lignans to enhance structural protection (as lignin precursors) and to protect against cavitation (Reyt et al. 2021), while accumulation of antioxidative flavonoids can enhance secondary oxidative stress tolerance (Nakabayashi et al., 2014). Moreover, under high Na_2SO_4, the sugar donor UDP-D-galactose increased alongside phenolic compounds, indicating a disruption in glycosylation and regulation of flavonoid bioactivity (Xiao et al., 2014). Similarly, increases in iridoid monoterpenoids, such as lamiide, under high Na_2SO_4 can support cell membrane integrity protection through prevention of lipid peroxidation (Delaporte et al., 2002). The high diversity of salt-responsive metabolites captured here implies additional functions beyond ROS scavenging, likely contributing to the observed Na_2SO_4 stress tolerance. For example, the reduction in sphingolipids, coherent with depleted octanoyl-CoA essential for their synthesis (Neess et al., 2015; Sonar et al., 2020), could play a role in limiting salt uptake below toxic thresholds as sphingolipids act as early sensors and signalling agents regulating ion transport (Jiang et al., 2019; Liu et al., 2022).

Primary metabolites declined in stems under both sulphur salt concentrations, including reductions in small peptides, saccharides, and nucleosides (Fig.5h). A slowdown of developmental processes and primary metabolism would be expected under salt stress, although there was no accompanying (short-term) impairment to total biomass production (Fig.2c). The comparatively limited disruption of secondary metabolites in stems suggests maintenance of homoeostasis and primary resource allocation to support root functions, effectively restricting salt stress propagation.

In leaves, the salt-responsive metabolites were broadly shared between both Na_2SO_4 levels, characterised by a large and dose-dependent accumulation (Fig.5f,g). This dose-dependent accumulation included saccharides, small peptides and precursors of phenolic compounds. Again, illustrating the buffering role of roots in protecting essential carbon fixation functions and energy-related compound production, even under severe salt exposure.

An increase of sulphur-containing compounds synthesis under SO_4^{2-} treatment and upregulation of sulphur assimilation and transport pathways is a characterised plant adaptation mechanism to effectively utilise excess SO_4^{2-} (Buchner et al., 2004; Davidian and Kopriva, 2010). Here, a substantial enrichment of small peptides occurred in roots under sulphur salinity (Fig.5h), with around half incorporating sulphur. This accumulation of

514 sulphur-containing compounds was consistent throughout the plant at both concentrations (Fig.5i) and was
515 predominantly cysteine and glutathione-based small peptides, some fatty acyl thioesters and alkaloids. The
516 integration of sulphate ions into organic sulphur-containing compounds has the potential to reduce ion
517 imbalance *in planta* during salt stress and could represent a tolerance mechanism in willow. Moreover, the
518 increase of structurally related compounds here (Fig.5i), although their functional information is limited in
519 plants, suggests activation of a bespoke, yet-to-be-described, metabolic response to Na_2SO_4. Watanabe et al.
520 (2019) highlighted a need for integrated sulphur-omics to overcome this shortfall in functional understanding
521 of sulphur-containing molecules in plants, of particular relevance to salinity tolerant non-model organisms such
522 as willow.

523 ***5.4 Salt anion identity shapes Salix metabolomic tolerance responses***

524 The salt response across all treatments involved an extensive proportion of the metabolome (28% of
525 metabolites), reflecting the highly plastic nature of plant metabolism under environmental change. While
526 activation of the calcium sensing signalling pathway by Na^+ (Munns and Tester, 2008) and disruption of the
527 Na^+/K^+ ratio (Zhang et al., 2018) are commonly considered to trigger salt responses in plants, anion driven
528 metabolomic responses have been less well explored. The comprehensive analysis of metabolic responses to
529 moderate NaCl and Na_2SO_4 treatments here, at equivalent soil electroconductivity and sodium concentrations,
530 revealed only 3% of metabolites were consistently responsive across both salt treatment, highlighting
531 extensive anion-specific changes (07).

532 The common, or generalised, salt metabolite changes were asymmetrically distributed across organs, with ~15-
533 fold more generalised salt responses in roots than in leaves (Fig.7b). This suggests common metabolic
534 strategies to tolerate (anion agnostic) osmotic stress in roots at the root-soil interface and restrict sodium
535 translocation, while leaves might be more susceptible to the (anion dependent) ion toxicity of translocated
536 Cl^- and SO_4^{2-}. The generalised salt response included common accumulation of the phenylpropanoid precursor
537 2-phenylacetamide in leaves (a salt biomarker in the euhalophyte *Suaeda salsa* (Bao et al., 2023)), protective
538 molecules in stems such as the anthocyanin ternatin C5 (Kovinich et al., 2015) and a highly antioxidative
539 coumaric acid conjugate of salicin, grandidentatin (Si et al., 2009), as well as potential cell wall structural
540 components in roots, such as the monolignol precursors syringin.

541 NaCl treatment, unlike Na_2SO_4, induced a comparatively small metabolomic response in leaves (Fig.6a-c). Of
542 the limited responses, a significant accumulation of spermidine, a polyamine known for its acid- and ROS-
543 neutralising properties, could help protect cell membranes, reduce chlorophyll loss and leaf senescence (Gill
544 and Tuteja, 2010b). The auxin conjugate, (indol-3-ylacetyl)-myo-inositol L-arabinoside, also increased,
545 suggesting oxidative stress specific developmental regulation (Bajguz and Piotrowska, 2009; Ludwig-Müller,
546 2011). A larger change under NaCl salt exposure was the reconfiguration of carbon resources through the
547 shikimate/phenylpropanoids pathway (Fig.6d,h). Specifically, lignans and phenylpropanoids displayed organ-
548 specific responses: substantial accumulation in roots and significant depletion in stems (Fig.6h). As major lignin
549 precursors, these lignan and phenylpropanoid dynamics could represent structural adaptations within the
550 roots and stems. In particular, lignin deposition can act as a barrier regulating ion uptake and translocation to
551 aerial parts (Byrt et al., 2018; Neves et al., 2010; Reyt et al., 2021).

552 Flavonoids, whose antioxidative capacity can facilitate localised neutralisation of reactive oxygen species
553 (Nakabayashi et al., 2014), also demonstrated marked organ-specific alteration, with substantial accumulation
554 in roots and dynamic regulation in the stems (Fig.6h). As flavonoids, phenolic acids, lignans and
555 phenylpropanoids all derive from the same substrates (phenylalanine and the pivotal intermediate cinnamic
556 acid), the organ-specific shift suggests a coordinated metabolic response promoting defence in the directly
557 exposed roots while simultaneously restricting the availability and energy expense of these compounds in the
558 stems. By comparison, moderate Na_2SO_4 did not induce similar extensive accumulation of phenolic compounds
559 in roots or stems but this response was triggered under higher Na_2SO_4 concentration.

560 Accumulation of osmoprotectants under salt stress is one of the most prevalent and well-described adaptive
561 strategies to reduce cell osmotic potential and stabilise cellular components (D'Amelia et al., 2018; Yang and
562 Guo, 2018). Surprisingly, except for stem proline enrichment under both NaCl and Na_2SO_4, the levels of
563 expected organic osmoprotectants, namely hydrophilic and low molecular weight sugars, polyamines or amino
564 acids, were largely reduced in roots and stems under NaCl while accumulating in leaves under Na_2SO_4, more
565 distal to the primary site of osmotic stress (Fig.5h, Fig.6f,g and Fig.7c). This response contrasts salt-tolerant

566 poplars which can accumulate soluble sugars as a tolerance mechanism (Jouve et al., 2004; Watanabe et al.,
567 2000) and might be a distinct strategy used by *S. miyabeana* to mitigate osmotic stress through the uptake of
568 inorganic ions, including root restricted Na^+ and anions (Cl^- and SO_4^{2-}) translocation to leaves. Similarly, Ottow
569 et al. (2005) reported preferential sodium uptake by *Populus euphratica*, where Na^+ served as a readily-
570 available osmoprotectant stored in the apoplast or bound in the cell wall, alongside reduced calcium and
571 soluble carbohydrate levels.

572 The anion-dependent regulation pattern of osmoprotectants also reflected broader differing metabolic
573 adjustments within central metabolism. Although reduction of stomatal conductance was similar between
574 both salts and photosystem II efficiency (Φ_{PSII}) preserved, the impact on foliar glucose and energy-related
575 compounds was distinct. NaCl was associated with the plant-wide reduction of glucose and multiple TCA cycle
576 intermediates (Supplementary – Fig.S8), representing impaired photosynthetic carbon fixation and decreased
577 flux through glycolysis and the TCA cycle, limiting mitochondrial respiration and overall energy supply. A similar
578 reconfiguration of resources and metabolic processes has been observed under salt stress in barley roots (Wu
579 et al., 2013), where glycolysis was inhibited, and in *Arabidopsis thalia* (Hartmann et al., 2015), where a shift to
580 non-oxidative fermentative energy metabolism can occur. This was coupled with reduced levels of small
581 peptides, nucleosides and other simple carbohydrates like fructose and sucrose in stems and roots (Fig.6f,g
582 and Fig.7c), possibly driven by increased carbon demand for secondary metabolism involved in salt stress
583 tolerance. By comparison, Na_2SO_4 induced an increase of glucose in leaves (Supplementary – Fig.S8), alongside
584 a distinct accumulation of saccharides, small peptides and nucleosides, consistent even under high Na_2SO_4. This
585 suggests that willow can sustain chemical energy production in leaves in the presence of sulphate, unlike with
586 chloride, and plant-wide production of salt-tolerance supporting metabolites, underscoring the importance of
587 understanding anion toxicity in salt tolerance and indicating a crucial role of excess sulphate incorporation into
588 organic compounds to prevent ionic imbalance. As an example, the accumulation of sulphur-containing
589 metabolites (Fig.5i,j), including 2,3-di-O-sulfopropylglucose, aligns with the mechanism of sugar sulphonation,
590 which can promote salt tolerance through ion regulation, osmotic tolerance, and cell wall integrity in algae
591 (Aquino et al., 2011).

592 Both chloride and sulphate salts activated the terpenoid pathway (Supplementary – Fig.S9), known to mitigate
593 salt stress in mangroves (Basyuni et al., 2009). NaCl induced significant accumulation of terpenoids from the
594 chloroplastic methylerythritol phosphate (MEP) pathway across the whole plant, including diterpenoids as well
595 as iridoid and secoiridoid monoterpenoids, comparable to transcriptomic changes observed in salt-tolerant
596 poplar (Chen et al., 2018). Na_2SO_4 treatment similarly enriched terpenoids through the MEP pathway, but
597 also activated the cytoplasmic mevalonate pathway in roots, also linked to salt tolerance in poplar (Wei et al.,
598 2020). This sulphate-salt-specific activation of the mevalonate pathway increased with higher Na_2SO_4 levels,
599 including enrichment of the hormone precursor abscisic aldehyde in roots and leaves. This suggests an adaptive
600 stress response where willows are positioned to quickly synthesise ABA, signalling stomatal closure, root
601 architecture changes, and osmoprotectant accumulation (Ryu and Cho, 2015), with ABA-aldehyde oxidase
602 mediated regulation. In contrast, ABA precursor enrichment was not observed with NaCl, which may leave
603 willows more vulnerable to salt stress, likely because chloride ions interfere with hormone signalling regulation
604 in the cytoplasm.

605 Overall, willow responded to salt stress by modulating both core and organ-specialised metabolites (Fig.4 and
606 Fig.7d). Within each organ, there was a tendency for greater depletion of organ-specialised compounds, over
607 core metabolites, indicating higher resilience of core metabolism under salt stress (Fig.7d). Contrasting this,
608 Na_2SO_4 treatment resulted in the enrichment of core metabolites in leaves, while NaCl rather enriched organ-
609 specialised compounds. Once again, this anion-specific difference highlights the nuanced metabolic
610 mechanisms deployed to face distinct salt stress conditions.

611 **6 Conclusion**

612 Untargeted metabolomics uncovered extremely high diversity of metabolites in willow, the majority of which
613 represent organ-specialised metabolites aligned with their distinct physiological function, but which also
614 include over 250 putative plant-wide stable, or core, metabolites. The leaves had the highest metabolite
615 diversity, but when subjected to different saline soil conditions, roots, as the frontline of exposure, had the
616 most extensive biochemical response, mitigating ion toxicity and osmotic pressure changes to enable plant

617 tolerance. However, the largely specialised nature of this response revealed that *in planta*, salt anion type
618 becomes an increasingly stronger discriminating force of metabolomic profile when moving from roots to
619 leaves. Indeed, the metabolic adjustment differed extensively in leaves, where Na_2SO_4 induces key components
620 of the core metabolome to mitigate complex osmotic and toxic stress even as soil salinity increases, whereas
621 NaCl induces more organ-specialised metabolic tools. Salinity levels in agriculture are currently categorised by
622 soil EC, however, given the substantial anion-dependent differences observed in plant metabolic responses,
623 soil EC measurement might be insufficient to reflect the diversity of soil salinity types, their actual osmotic
624 potential, as well as the anion-specific plant metabolic toolkit necessary for plant salt tolerance.

625 **7 Declaration of Competing Interest**

626 The authors declare that there is no conflict of interest.

627 **8 Acknowledgements**

628 We gratefully acknowledge the financial support provided from NSERC Discovery Grants (RGPIN-2017-05452
629 and RGPIN-2023-04863), Natural Resources Canada Forest Innovation Program Grant (CWFC1718-018 and
630 CWFC1920-104), ECCC Environmental Damage Fund (EDF-PQ-2020b012), MITACS (IT23193), and the UCD Ad
631 Astra Award Program. A special thank you is extended to Ariane Lafrenière, Marc-Olivier Brunette and Bruno
632 Guerrier for their kind and effective support during harvest, and to Allan Harms from NRAL, University of
633 Alberta, for his valuable expertise and sympathy.

634 **9 Data availability statement**

635 The data that supports the findings of this study are available in the supplementary material of this article.

636 **10 References**

637 Abdelgadir, E.M., Oka, M., Fujiyama, H., 2005. Characteristics of Nitrate Uptake by Plants Under Salinity. J. Plant
638 Nutr. 28, 33–46. https://doi.org/10.1081/PLN-200042156
639 Abreu, M., Silva, L., Ribeiro, B., Ferreira, A., Alves, L., Paixão, S.M., Gouveia, L., Moura, P., Carvalheiro, F.,
640 Duarte, L.C., Fernando, A.L., Reis, A., Gírio, F., 2022. Q-Low indirect land use change (ILUC) energy crops
641 to bioenergy and biofuels: A review. Energies 15, 4348. https://doi.org/10.3390/en15124348
642 Aliferis, K.A., Chamoun, R., Jabaji, S., 2015. Metabolic responses of willow (Salix purpurea L.) leaves to
643 mycorrhization as revealed by mass spectrometry and 1H NMR spectroscopy metabolite profiling.
644 Front. Plant Sci. 6.
645 Alseekh, S., Aharoni, A., Brotman, Y., Contrepois, K., D'Auria, J., Ewald, J., C. Ewald, J., Fraser, P.D., Giavalisco,
646 P., Hall, R.D., Heinemann, M., Link, H., Luo, J., Neumann, S., Nielsen, J., Perez de Souza, L., Saito, K.,
647 Sauer, U., Schroeder, F.C., Schuster, S., Siuzdak, G., Skirycz, A., Sumner, L.W., Snyder, M.P., Tang, H.,
648 Tohge, T., Wang, Y., Wen, W., Wu, S., Xu, G., Zamboni, N., Fernie, A.R., 2021. Mass spectrometry-based
649 metabolomics: a guide for annotation, quantification and best reporting practices. Nat. Methods 18,
650 747–756. https://doi.org/10.1038/s41592-021-01197-1
651 Aquino, R.S., Grativol, C., Mourão, P.A.S., 2011. Rising from the Sea: Correlations between Sulfated
652 Polysaccharides and Salinity in Plants. PLOS ONE 6, e18862.
653 https://doi.org/10.1371/journal.pone.0018862
654 Arif, Y., Singh, P., Siddiqui, H., Bajguz, A., Hayat, S., 2020. Salinity induced physiological and biochemical changes
655 in plants: An omic approach towards salt stress tolerance. Plant Physiol. Biochem. 156, 64–77.
656 https://doi.org/10.1016/j.plaphy.2020.08.042
657 Badri, D.V., Vivanco, J.M., 2009. Q-Regulation and function of root exudates. Plant Cell Environ. 32, 666–681.
658 https://doi.org/10.1111/j.1365-3040.2009.01926.x
659 Bajguz, A., Piotrowska, A., 2009. Conjugates of auxin and cytokinin. Phytochemistry 70, 957–969.
660 https://doi.org/10.1016/j.phytochem.2009.05.006
661 Bao, J., Liu, Z., Ding, Z., Yisilam, G., Wang, Q., Tian, X., Bao, J., Liu, Z., Ding, Z., Yisilam, G., Wang, Q., Tian, X.,
662 2023. Metabolomic analysis reveals key metabolites and metabolic pathways in Suaeda salsa under
663 salt and drought stress. Funct. Plant Biol. https://doi.org/10.1071/FP23049

Basyuni, M., Baba, S., Inafuku, M., Iwasaki, H., Kinjo, K., Oku, H., 2009. Q-Expression of terpenoid synthase mRNA and terpenoid content in salt stressed mangrove. J. Plant Physiol. 166, 1786–1800. https://doi.org/10.1016/j.jplph.2009.05.008

Bilek, M.A., Soolanayakanahally, R.Y., Guy, R.D., Mansfield, S.D., 2020. Q-Physiological response of *Populus balsamifera* and *Salix eriocephala* to salinity and hydraulic fracturing wastewater: potential for phytoremediation applications. Int. J. Environ. Res. Public. Health 17, 7641. https://doi.org/10.3390/ijerph17207641

Boeckler, G.A., Gershenzon, J., Unsicker, S.B., 2011. Phenolic glycosides of the Salicaceae and their role as anti-herbivore defenses. Phytochemistry, Plant-Insect Interactions 72, 1497–1509. https://doi.org/10.1016/j.phytochem.2011.01.038

Brereton, N.J.B., Berthod, N., Lafleur, B., Pedneault, K., Pitre, F.E., Labrecque, M., 2017. Extractable phenolic yield variation in five cultivars of mature short rotation coppice willow from four plantations in Quebec. Ind. Crops Prod. 97, 525–535. https://doi.org/10.1016/j.indcrop.2016.12.049

Buchner, P., Takahashi, H., Hawkesford, M.J., 2004. Plant sulphate transporters: co-ordination of uptake, intracellular and long-distance transport. J. Exp. Bot. 55, 1765–1773. https://doi.org/10.1093/jxb/erh206

Buer, C.S., Imin, N., Djordjevic, M.A., 2010. Flavonoids: New Roles for Old Molecules. J. Integr. Plant Biol. 52, 98–111. https://doi.org/10.1111/j.1744-7909.2010.00905.x

Byrt, C.S., Munns, R., Burton, R.A., Gilliham, M., Wege, S., 2018. Q-Root cell wall solutions for crop plants in saline soils. Plant Sci. 269, 47–55. https://doi.org/10.1016/j.plantsci.2017.12.012

Cesco, S., Mimmo, T., Tonon, G., Tomasi, N., Pinton, R., Terzano, R., Neumann, G., Weisskopf, L., Renella, G., Landi, L., Nannipieri, P., 2012. Plant-borne flavonoids released into the rhizosphere: impact on soil bio-activities related to plant nutrition. A review. Biol. Fertil. Soils 48, 123–149. https://doi.org/10.1007/s00374-011-0653-2

Chambers, M.C., Maclean, B., Burke, R., Amodei, D., Ruderman, D.L., Neumann, S., Gatto, L., Fischer, B., Pratt, B., Egertson, J., Hoff, K., Kessner, D., Tasman, N., Shulman, N., Frewen, B., Baker, T.A., Brusniak, M.-Y., Paulse, C., Creasy, D., Flashner, L., Kani, K., Moulding, C., Seymour, S.L., Nuwaysir, L.M., Lefebvre, B., Kuhlmann, F., Roark, J., Rainer, P., Detlev, S., Hemenway, T., Huhmer, A., Langridge, J., Connolly, B., Chadick, T., Holly, K., Eckels, J., Deutsch, E.W., Moritz, R.L., Katz, J.E., Agus, D.B., MacCoss, M., Tabb, D.L., Mallick, P., 2012. A cross-platform toolkit for mass spectrometry and proteomics. Nat. Biotechnol. 30, 918–920. https://doi.org/10.1038/nbt.2377

Chan, K.X., Phua, S.Y., Van Breusegem, F., 2019. Secondary sulfur metabolism in cellular signalling and oxidative stress responses. J. Exp. Bot. 70, 4237–4250. https://doi.org/10.1093/jxb/erz119

Chen, P., Zuo, L., Yu, X., Dong, Y., Zhang, S., Yang, M., 2018. Response mechanism in Populus × euramericana cv. '74/76' revealed by RNA-seq under salt stress. Acta Physiol. Plant. 40, 96. https://doi.org/10.1007/s11738-018-2676-x

Chen, S., Polle, A., 2010. Salinity tolerance of Populus. Plant Biol. 12, 317–333. https://doi.org/10.1111/j.1438-8677.2009.00301.x

Corwin, D.L., Scudiero, E., 2019. Chapter One - Review of soil salinity assessment for agriculture across multiple scales using proximal and/or remote sensors, in: Sparks, D.L. (Ed.), Advances in Agronomy. Academic Press, pp. 1–130. https://doi.org/10.1016/bs.agron.2019.07.001

D'Amelia, L., Dell'Aversana, E., Woodrow, P., Ciarmiello, L.F., Carillo, P., 2018. Metabolomics for Crop Improvement Against Salinity Stress, in: Kumar, V., Wani, S.H., Suprasanna, P., Tran, L.-S.P. (Eds.), Salinity Responses and Tolerance in Plants, Volume 2: Exploring RNAi, Genome Editing and Systems Biology. Springer International Publishing, Cham, pp. 267–287. https://doi.org/10.1007/978-3-319-90318-7_11

Davidian, J.-C., Kopriva, S., 2010. Regulation of Sulfate Uptake and Assimilation—the Same or Not the Same? Mol. Plant 3, 314–325. https://doi.org/10.1093/mp/ssq001

De Vos, R.C., Moco, S., Lommen, A., Keurentjes, J.J., Bino, R.J., Hall, R.D., 2007. Untargeted large-scale plant metabolomics using liquid chromatography coupled to mass spectrometry. Nat. Protoc. 2, 778–791. https://doi.org/10.1038/nprot.2007.95

Deinlein, U., Stephan, A.B., Horie, T., Luo, W., Xu, G., Schroeder, J.I., 2014. Q-Plant salt-tolerance mechanisms. Trends Plant Sci. 19, 371–379. https://doi.org/10.1016/j.tplants.2014.02.001

Delaporte, R.H., Sánchez, G.M., Cuellar, A.C., Giuliani, A., Palazzo de Mello, J.C., 2002. Anti-inflammatory activity and lipid peroxidation inhibition of iridoid lamiide isolated from Bouchea fluminensis (Vell.) Mold. (Verbenaceae). J. Ethnopharmacol. 82, 127–130. https://doi.org/10.1016/S0378-8741(02)00181-2

Dick, W.A., Kost, D., Chen, L., 2008. Availability of Sulfur to Crops from Soil and Other Sources, in: Sulfur: A Missing Link between Soils, Crops, and Nutrition. John Wiley & Sons, Ltd, pp. 59–82. https://doi.org/10.2134/agronmonogr50.c5

Dimitriou, I., Aronsson, P., 2005. Willows for energy and phytoremediation in Sweden 56.

Drapal, M., Enfissi, E.M.A., Fraser, P.D., 2022. The chemotype core collection of genus Nicotiana. Plant J. 110, 1516–1528. https://doi.org/10.1111/tpj.15745

Dührkop, K., Fleischauer, M., Ludwig, M., Aksenov, A.A., Melnik, A.V., Meusel, M., Dorrestein, P.C., Rousu, J., Böcker, S., 2019. SIRIUS 4: a rapid tool for turning tandem mass spectra into metabolite structure information. Nat. Methods 16, 299–302. https://doi.org/10.1038/s41592-019-0344-8

Dührkop, K., Nothias, L.F., Fleischauer, M., Ludwig, M., Hoffmann, M.A., Rousu, J., Dorrestein, P.C., Böcker, S., 2020. Classes for the masses: Systematic classification of unknowns using fragmentation spectra. https://doi.org/10.1101/2020.04.17.046672

Dussarrat, T., Prigent, S., Latorre, C., Bernillon, S., Flandin, A., Díaz, F.P., Cassan, C., Van Delft, P., Jacob, D., Varala, K., Joubes, J., Gibon, Y., Rolin, D., Gutiérrez, R.A., Pétriacq, P., 2022. Predictive metabolomics of multiple Atacama plant species unveils a core set of generic metabolites for extreme climate resilience. New Phytol. 234, 1614–1628. https://doi.org/10.1111/nph.18095

Endo, I., Kobatake, M., Tanikawa, N., Nakaji, T., Ohashi, M., Makita, N., 2021. Anatomical patterns of condensed tannin in fine roots of tree species from a cool-temperate forest. Ann. Bot. 128, 59–71. https://doi.org/10.1093/aob/mcab022

Evelin, H., Kapoor, R., Giri, B., 2009. Q-Arbuscular mycorrhizal fungi in alleviation of salt stress: a review. Ann. Bot. 104, 1263–1280. https://doi.org/10.1093/aob/mcp251

FAO (Ed.), 2015. Status of the World's Soil Resources: Main Report.

FAO (Ed.), 1988. Salt-affected Soils and Their Management, FAO Soils Bulletin 39.

Franco-Navarro, J.D., Brumós, J., Rosales, M.A., Cubero-Font, P., Talón, M., Colmenero-Flores, J.M., 2016. Chloride regulates leaf cell size and water relations in tobacco plants. J. Exp. Bot. 67, 873–891. https://doi.org/10.1093/jxb/erv502

Geilfus, C.-M., 2018. Chloride: from Nutrient to Toxicant. Plant Cell Physiol. 59, 877–886. https://doi.org/10.1093/pcp/pcy071

Genty, B., Briantais, J.-M., Baker, N.R., 1989. The relationship between the quantum yield of photosynthetic electron transport and quenching of chlorophyll fluorescence. Biochim. Biophys. Acta BBA - Gen. Subj. 990, 87–92. https://doi.org/10.1016/S0304-4165(89)80016-9

Gil-de-la-Fuente, A., Godzien, J., Saugar, S., Garcia-Carmona, R., Badran, H., Wishart, D.S., Barbas, C., Otero, A., 2019. CEU Mass Mediator 3.0: A Metabolite Annotation Tool. J. Proteome Res. 18, 797–802. https://doi.org/10.1021/acs.jproteome.8b00720

Gill, S.S., Tuteja, N., 2010a. Reactive oxygen species and antioxidant machinery in abiotic stress tolerance in crop plants. Plant Physiol. Biochem. 48, 909–930. https://doi.org/10.1016/J.PLAPHY.2010.08.016

Gill, S.S., Tuteja, N., 2010b. Polyamines and abiotic stress tolerance in plants. Plant Signal. Behav. 5, 26–33. https://doi.org/10.4161/psb.5.1.10291

Gonzalez, E., Pitre, F.E., Pagé, A.P., Marleau, J., Guidi Nissim, W., St-Arnaud, M., Labrecque, M., Joly, S., Yergeau, E., Brereton, N.J.B., 2018. Trees, fungi and bacteria: tripartite metatranscriptomics of a root microbiome responding to soil contamination. Microbiome 6, 53. https://doi.org/10.1186/s40168-018-0432-5

Guignard, C., Jouve, L., Bogéat-Triboulot, M.B., Dreyer, E., Hausman, J.-F., Hoffmann, L., 2005. Analysis of carbohydrates in plants by high-performance anion-exchange chromatography coupled with electrospray mass spectrometry. J. Chromatogr. A, 17th International Ion Chromatography Symposium 1085, 137–142. https://doi.org/10.1016/j.chroma.2005.05.068

Guo, R., Shi, L., Yan, C., Zhong, X., Gu, F., Liu, Q., Xia, X., Li, H., 2017. Ionomic and metabolic responses to neutral salt or alkaline salt stresses in maize (Zea mays L.) seedlings. BMC Plant Biol. 17, 41. https://doi.org/10.1186/s12870-017-0994-6

770 Gupta, B., Huang, B., 2014. Q-Mechanism of salinity tolerance in plants: physiological, biochemical, and
771 molecular characterization. Int. J. Genomics 2014, 701596–701596.
772 https://doi.org/10.1155/2014/701596
773 Hangs, R.D., Schoenau, J.J., Van Rees, K.C.J., Steppuhn, H., 2011. Examining the salt tolerance of willow (Salix
774 spp.) bioenergy species for use on salt-affected agricultural lands. Can. J. Plant Sci. 91, 509–517.
775 https://doi.org/10.4141/cjps10135
776 Hartmann, L., Pedrotti, L., Weiste, C., Fekete, A., Schierstaedt, J., Göttler, J., Kempa, S., Krischke, M., Dietrich,
777 K., Mueller, M.J., Vicente-Carbajosa, J., Hanson, J., Dröge-Laser, W., 2015. Crosstalk between Two bZIP
778 Signaling Pathways Orchestrates Salt-Induced Metabolic Reprogramming in Arabidopsis Roots. Plant
779 Cell 27, 2244–2260. https://doi.org/10.1105/tpc.15.00163
780 Hassani, A., Azapagic, A., Shokri, N., 2021. Global predictions of primary soil salinization under changing climate
781 in the 21st century. Nat. Commun. 12, 6663. https://doi.org/10.1038/s41467-021-26907-3
782 Hauser, F., Horie, T., 2010. A conserved primary salt tolerance mechanism mediated by HKT transporters: a
783 mechanism for sodium exclusion and maintenance of high K+/Na+ ratio in leaves during salinity stress.
784 Plant Cell Environ. 33, 552–565. https://doi.org/10.1111/j.1365-3040.2009.02056.x
785 Hawkins, C., Ginzburg, D., Zhao, K., Dwyer, W., Xue, B., Xu, A., Rice, S., Cole, B., Paley, S., Karp, P., Rhee, S.Y.,
786 2021. Plant Metabolic Network 15: A resource of genome-wide metabolism databases for 126 plants
787 and algae. J. Integr. Plant Biol. 63, 1888–1905. https://doi.org/10.1111/jipb.13163
788 He, H., Tang, W., Wang, W., Crits-Christoph, P., 2014. Structural zeroes and zero-inflated models. Shanghai
789 Arch. Psychiatry 26, 236–242. https://doi.org/10.3969/j.issn.1002-0829.2014.04.008
790 Hillabrand, R.M., Gordon, H., Hynes, B., Constabel, C.P., Landhäusser, S.M., 2023. Populus root salicinoid
791 phenolic glycosides are not mobilized to support metabolism and regrowth under carbon-limited
792 conditions. Tree Physiol. tpad020. https://doi.org/10.1093/treephys/tpad020
793 Huang, X., Hefer, C.A., Soolanayakanahally, R.Y., Guy, R.D., Mansfield, S.D., 2023. The Overlooked Ion:
794 Unraveling the Effects of Magnesium-Specific Toxicity on Willows Under Sulphate Salinity. Environ. Exp.
795 Bot. 105634. https://doi.org/10.1016/j.envexpbot.2023.105634
796 Huang, X., Soolanayakanahally, R.Y., Guy, R.D., Shunmugam, A.S.K., Mansfield, S.D., 2020. Differences in growth
797 and physiological and metabolic responses among Canadian native and hybrid willows (Salix spp.)
798 under salinity stress. Tree Physiol. 40, 652–666. https://doi.org/10.1093/treephys/tpaa017
799 Huber, F., Ridder, L., Verhoeven, S., Spaaks, J.H., Diblen, F., Rogers, S., Hooft, J.J.J. van der, 2021. Spec2Vec:
800 Improved mass spectral similarity scoring through learning of structural relationships. PLOS Comput.
801 Biol. 17, e1008724. https://doi.org/10.1371/journal.pcbi.1008724
802 Huby, E., Napier, J.A., Baillieul, F., Michaelson, L.V., Dhondt-Cordelier, S., 2020. Sphingolipids: towards an
803 integrated view of metabolism during the plant stress response. New Phytol. 225, 659–670.
804 https://doi.org/10.1111/nph.15997
805 Ifuku, K., 2015. Localization and functional characterization of the extrinsic subunits of photosystem II: an
806 update. Biosci. Biotechnol. Biochem. 79, 1223–1231.
807 https://doi.org/10.1080/09168451.2015.1031078
808 Janz, D., Lautner, S., Wildhagen, H., Behnke, K., Schnitzler, J.-P., Rennenberg, H., Fromm, J., Polle, A., 2012. Salt
809 stress induces the formation of a novel type of 'pressure wood' in two Populus species. New Phytol.
810 194, 129–141. https://doi.org/10.1111/j.1469-8137.2011.03975.x
811 Jerbi, A., Brereton, N.J.B., Sas, E., Amiot, S., Lachapelle-T., X., Comeau, Y., Pitre, F.E., Labrecque, M., 2020. High
812 biomass yield increases in a primary effluent wastewater phytofiltration are associated to altered leaf
813 morphology and stomatal size in Salix miyabeana. Sci. Total Environ. 738, 139728.
814 https://doi.org/10.1016/j.scitotenv.2020.139728
815 Jia, H., Wang, L., Li, J., Sun, P., Lu, M., Hu, J., 2020. Comparative metabolomics analysis reveals different
816 metabolic responses to drought in tolerant and susceptible poplar species. Physiol. Plant. 168, 531–
817 546. https://doi.org/10.1111/ppl.13036
818 Jiang, Z., Zhou, X., Tao, M., Yuan, F., Liu, L., Wu, F., Wu, X., Xiang, Y., Niu, Y., Liu, F., Li, C., Ye, R., Byeon, B., Xue,
819 Y., Zhao, H., Wang, H.-N., Crawford, B.M., Johnson, D.M., Hu, C., Pei, C., Zhou, W., Swift, G.B., Zhang,
820 H., Vo-Dinh, T., Hu, Z., Siedow, J.N., Pei, Z.-M., 2019. Plant cell-surface GIPC sphingolipids sense salt to
821 trigger Ca2+ influx. Nature 572, 341–346. https://doi.org/10.1038/s41586-019-1449-z

822 Jouve, L., Hoffmann, L., Hausman, J.-F., 2004. Polyamine, Carbohydrate, and Proline Content Changes During
823 Salt Stress Exposure of Aspen (Populus tremula L.): Involvement of Oxidation and Osmoregulation
824 Metabolism. Plant Biol. 6, 74–80. https://doi.org/10.1055/s-2003-44687
825 Kaling, M., Kanawati, B., Ghirardo, A., Albert, A., Winkler, J.B., Heller, W., Barta, C., Loreto, F., Schmitt-Kopplin,
826 P., Schnitzler, J.-P., 2015. UV-B mediated metabolic rearrangements in poplar revealed by non-targeted
827 metabolomics. Plant Cell Environ. 38, 892–904. https://doi.org/10.1111/pce.12348
828 Karpievitch, Y.V., Nikolic, S.B., Wilson, R., Sharman, J.E., Edwards, L.M., 2014. Metabolomics data normalization
829 with EigenMS. PloS One 9, e116221. https://doi.org/10.1371/journal.pone.0116221
830 Kim, H.W., Wang, M., Leber, C.A., Nothias, L.-F., Reher, R., Kang, K.B., van der Hooft, J.J.J., Dorrestein, P.C.,
831 Gerwick, W.H., Cottrell, G.W., 2021. NPClassifier: A Deep Neural Network-Based Structural
832 Classification Tool for Natural Products. J. Nat. Prod. 84, 2795–2807.
833 https://doi.org/10.1021/acs.jnatprod.1c00399
834 Köhler, A., Förster, N., Zander, M., Ulrichs, C., 2020. Compound-specific responses of phenolic metabolites in
835 the bark of drought-stressed Salix daphnoides and Salix purpurea. Plant Physiol. Biochem. 155, 311–
836 320. https://doi.org/10.1016/j.plaphy.2020.07.004
837 Kovinich, N., Kayanja, G., Chanoca, A., Otegui, M.S., Grotewold, E., 2015. Abiotic stresses induce different
838 localizations of anthocyanins in Arabidopsis. Plant Signal. Behav. 10, e1027850.
839 https://doi.org/10.1080/15592324.2015.1027850
840 Li, D., Heiling, S., Baldwin, I.T., Gaquerel, E., 2016. Illuminating a plant's tissue-specific metabolic diversity using
841 computational metabolomics and information theory. Proc. Natl. Acad. Sci. 113, E7610–E7618.
842 https://doi.org/10.1073/pnas.1610218113
843 Litalien, A., Zeeb, B., 2020. Curing the earth: A review of anthropogenic soil salinization and plant-based
844 strategies for sustainable mitigation. Sci. Total Environ. 698, 134235.
845 https://doi.org/10.1016/j.scitotenv.2019.134235
846 Liu, Y., Wang, L., Li, X., Luo, M., 2022. Detailed sphingolipid profile responded to salt stress in cotton root and
847 the GhIPCS1 is involved in the regulation of plant salt tolerance. Plant Sci. 316, 111174.
848 https://doi.org/10.1016/j.plantsci.2021.111174
849 Llanes, A., Bertazza, G., Palacio, G., Luna, V., 2013. Different sodium salts cause different solute accumulation
850 in the halophyte Prosopis strombulifera. Plant Biol. 15, 118–125. https://doi.org/10.1111/j.1438-
851 8677.2012.00626.x
852 Ludwig-Müller, J., 2011. Auxin conjugates: their role for plant development and in the evolution of land plants.
853 J. Exp. Bot. 62, 1757–1773. https://doi.org/10.1093/jxb/erq412
854 Major, J.E., Mosseler, A., Malcolm, J.W., 2017. Salix species variation in leaf gas exchange, sodium, and nutrient
855 parameters at three levels of salinity. Can. J. For. Res. 47, 1045–1055. https://doi.org/10.1139/cjfr-
856 2017-0028
857 McLaughlin, S., Zhalnina, K., Kosina, S., Northen, T.R., Sasse, J., 2023. The core metabolome and root exudation
858 dynamics of three phylogenetically distinct plant species. Nat. Commun. 14, 1649.
859 https://doi.org/10.1038/s41467-023-37164-x
860 Meier, B., Julkunen-Tiitto, R., Tahvanainen, J., Sticher, O., 1988. Comparative high-performance liquid and gas-
861 liquid chromatographic determination of phenolic glucosides in salicaceae species. J. Chromatogr. A
862 442, 175–186. https://doi.org/10.1016/S0021-9673(00)94467-4
863 Mirck, J., Zalesny, R.S., 2015. Mini-Review of Knowledge Gaps in Salt Tolerance of Plants Applied to Willows
864 and Poplars. Int. J. Phytoremediation 17, 640–650. https://doi.org/10.1080/15226514.2014.950414
865 Munns, R., 2002. Comparative physiology of salt and water stress. Plant Cell Environ. 25, 239–250.
866 https://doi.org/10.1046/j.0016-8025.2001.00808.x
867 Munns, R., Day, D.A., Fricke, W., Watt, M., Arsova, B., Barkla, B.J., Bose, J., Byrt, C.S., Chen, Z.-H., Foster, K.J.,
868 Gilliham, M., Henderson, S.W., Jenkins, C.L.D., Kronzucker, H.J., Miklavcic, S.J., Plett, D., Roy, S.J.,
869 Shabala, S., Shelden, M.C., Soole, K.L., Taylor, N.L., Tester, M., Wege, S., Wegner, L.H., Tyerman, S.D.,
870 2020a. Energy costs of salt tolerance in crop plants. New Phytol. 225, 1072–1090.
871 https://doi.org/10.1111/nph.15864
872 Munns, R., Passioura, J.B., Colmer, T.D., Byrt, C.S., 2020b. Q-Osmotic adjustment and energy limitations to plant
873 growth in saline soil. New Phytol. 225, 1091–1096. https://doi.org/10.1111/nph.15862
874 Munns, R., Tester, M., 2008. Mechanisms of Salinity Tolerance. Annu. Rev. Plant Biol. 59, 651–681.
875 https://doi.org/10.1146/annurev.arplant.59.032607.092911

Nakabayashi, R., Yonekura-Sakakibara, K., Urano, K., Suzuki, M., Yamada, Y., Nishizawa, T., Matsuda, F., Kojima, M., Sakakibara, H., Shinozaki, K., Michael, A.J., Tohge, T., Yamazaki, M., Saito, K., 2014. Enhancement of oxidative and drought tolerance in Arabidopsis by overaccumulation of antioxidant flavonoids. Plant J. 77, 367–379. https://doi.org/10.1111/tpj.12388

Neess, D., Bek, S., Engelsby, H., Gallego, S.F., Færgeman, N.J., 2015. Long-chain acyl-CoA esters in metabolism and signaling: Role of acyl-CoA binding proteins. Prog. Lipid Res. 59, 1–25. https://doi.org/10.1016/j.plipres.2015.04.001

Neves, G.Y.S., Marchiosi, R., Ferrarese, M.L.L., Siqueira-Soares, R.C., Ferrarese-Filho, O., 2010. Root Growth Inhibition and Lignification Induced by Salt Stress in Soybean. J. Agron. Crop Sci. 196, 467–473. https://doi.org/10.1111/j.1439-037X.2010.00432.x

Nguyen, H.T., Meir, P., Sack, L., Evans, J.R., Oliveira, R.S., Ball, M.C., 2017. Leaf water storage increases with salinity and aridity in the mangrove Avicennia marina: integration of leaf structure, osmotic adjustment and access to multiple water sources. Plant Cell Environ. 40, 1576–1591. https://doi.org/10.1111/pce.12962

Nothias, L.-F., Petras, D., Schmid, R., Dührkop, K., Rainer, J., Sarvepalli, A., Protsyuk, I., Ernst, M., Tsugawa, H., Fleischauer, M., Aicheler, F., Aksenov, A.A., Alka, O., Allard, P.-M., Barsch, A., Cachet, X., Caraballo-Rodriguez, A.M., Da Silva, R.R., Dang, T., Garg, N., Gauglitz, J.M., Gurevich, A., Isaac, G., Jarmusch, A.K., Kameník, Z., Kang, K.B., Kessler, N., Koester, I., Korf, A., Le Gouellec, A., Ludwig, M., Martin H., C., McCall, L.-I., McSayles, J., Meyer, S.W., Mohimani, H., Morsy, M., Moyne, O., Neumann, S., Neuweger, H., Nguyen, N.H., Nothias-Esposito, M., Paolini, J., Phelan, V.V., Pluskal, T., Quinn, R.A., Rogers, S., Shrestha, B., Tripathi, A., van der Hooft, J.J.J., Vargas, F., Weldon, K.C., Witting, M., Yang, H., Zhang, Z., Zubeil, F., Kohlbacher, O., Böcker, S., Alexandrov, T., Bandeira, N., Wang, M., Dorrestein, P.C., 2020. Feature-based molecular networking in the GNPS analysis environment. Nat. Methods 17, 905–908. https://doi.org/10.1038/s41592-020-0933-6

Osawa, H., Endo, I., Hara, Y., Matsushima, Y., Tange, T., 2011. Transient Proliferation of Proanthocyanidin-Accumulating Cells on the Epidermal Apex Contributes to Highly Aluminum-Resistant Root Elongation in Camphor Tree. Plant Physiol. 155, 433–446. https://doi.org/10.1104/pp.110.166967

Ottow, E.A., Brinker, M., Teichmann, T., Fritz, E., Kaiser, W., Brosché, M., Kangasjärvi, J., Jiang, X., Polle, A., 2005. Populus euphratica Displays Apoplastic Sodium Accumulation, Osmotic Adjustment by Decreases in Calcium and Soluble Carbohydrates, and Develops Leaf Succulence under Salt Stress. Plant Physiol. 139, 1762–1772. https://doi.org/10.1104/pp.105.069971

Pichersky, E., Raguso, R.A., 2018. Why do plants produce so many terpenoid compounds? New Phytol. 220, 692–702. https://doi.org/10.1111/nph.14178

Pobłocka-Olech, L., van Nederkassel, A.-M., Vander Heyden, Y., Krauze-Baranowska, M., Glód, D., Baczek, T., 2007. Chromatographic analysis of salicylic compounds in different species of the genus Salix. J. Sep. Sci. 30, 2958–2966. https://doi.org/10.1002/jssc.200700137

Polle, A., Chen, S., 2015. On the salty side of life: molecular, physiological and anatomical adaptation and acclimation of trees to extreme habitats. Plant Cell Environ. 38, 1794–1816. https://doi.org/10.1111/pce.12440

Prasad, R., Shivay, Y.S., 2018. Sulphur in Soil, Plant and Human Nutrition. Proc. Natl. Acad. Sci. India Sect. B Biol. Sci. 88, 429–434. https://doi.org/10.1007/s40011-016-0769-0

Quinn, L.D., Straker, K.C., Guo, J., Kim, S., Thapa, S., Kling, G., Lee, D.K., Voigt, T.B., 2015. Q-Stress-tolerant feedstocks for sustainable bioenergy production on marginal land. BioEnergy Res. 8, 1081–1100. https://doi.org/10.1007/s12155-014-9557-y

R Core Team, 2022. R: A Language and environment for statistical computing.

Rausch, T., Wachter, A., 2005. Sulfur metabolism: a versatile platform for launching defence operations. Trends Plant Sci. 10, 503–509. https://doi.org/10.1016/j.tplants.2005.08.006

Reginato, M., Luna, V., Papenbrock, J., 2021. Current knowledge about Na2SO4 effects on plants: what is different in comparison to NaCl? J. Plant Res. 134, 1159–1179. https://doi.org/10.1007/s10265-021-01335-y

Reginato, M.A., Turcios, A.E., Luna, V., Papenbrock, J., 2019. Differential effects of NaCl and Na2SO4 on the halophyte Prosopis strombulifera are explained by different responses of photosynthesis and metabolism. Plant Physiol. Biochem. 141, 306–314. https://doi.org/10.1016/j.plaphy.2019.05.027

Reich, M., Aghajanzadeh, T., Helm, J., Parmar, S., Hawkesford, M.J., De Kok, L.J., 2017. Chloride and sulfate salinity differently affect biomass, mineral nutrient composition and expression of sulfate transport and assimilation genes in Brassica rapa. Plant Soil 411, 319–332. https://doi.org/10.1007/s11104-016-3026-7

Reyt, G., Ramakrishna, P., Salas-González, I., Fujita, S., Love, A., Tiemessen, D., Lapierre, C., Morreel, K., Calvo-Polanco, M., Flis, P., Geldner, N., Boursiac, Y., Boerjan, W., George, M.W., Castrillo, G., Salt, D.E., 2021. Two chemically distinct root lignin barriers control solute and water balance. Nat. Commun. 12, 2320. https://doi.org/10.1038/s41467-021-22550-0

Richter, J.A., Behr, J.H., Erban, A., Kopka, J., Zörb, C., 2019. Ion-dependent metabolic responses of Vicia faba L. to salt stress. Plant Cell Environ. 42, 295–309. https://doi.org/10.1111/pce.13386

Rodriguez, H.G., Roberts, JKM., Jordan, W.R., Drew, M.C., 1997. Q-Growth, water relations, and accumulation of organic and inorganic solutes in roots of maize seedlings during salt stress. Plant Physiol. 113, 881–893. https://doi.org/10.1104/pp.113.3.881

Rodzkin, A., Volk, T., 2018. Using schrub willow for biological reclamation of areas with raised soil salinity.

Rohart, F., Gautier, B., Singh, A., Cao, K.-A.L., 2017. mixOmics: An R package for 'omics feature selection and multiple data integration. PLOS Comput. Biol. 13, e1005752. https://doi.org/10.1371/journal.pcbi.1005752

Ruuhola, T., Julkunen-Tiitto, R., 2003. Trade-Off Between Synthesis of Salicylates and Growth of Micropropagated Salix pentandra. J. Chem. Ecol. 29, 1565–1588. https://doi.org/10.1023/A:1024266612585

Ryu, H., Cho, Y.-G., 2015. Q-Plant hormones in salt stress tolerance. J. Plant Biol. 58, 147–155. https://doi.org/10.1007/s12374-015-0103-z

Sanchez, D.H., Siahpoosh, M.R., Roessner, U., Udvardi, M., Kopka, J., 2008. Plant metabolomics reveals conserved and divergent metabolic responses to salinity. Physiol. Plant. 132, 209–219. https://doi.org/10.1111/j.1399-3054.2007.00993.x

Sas, E., Hennequin, L.M., Frémont, A., Jerbi, A., Legault, N., Lamontagne, J., Fagoaga, N., Sarrazin, M., Hallett, J.P., Fennell, P.S., Barnabé, S., Labrecque, M., Brereton, N.J.B., Pitre, F.E., 2021. Biorefinery potential of sustainable municipal wastewater treatment using fast-growing willow. Sci. Total Environ. 792, 148146. https://doi.org/10.1016/j.scitotenv.2021.148146

Sasse, J., Martinoia, E., Northen, T., 2018. Feed Your Friends: Do Plant Exudates Shape the Root Microbiome? Trends Plant Sci. 23, 25–41. https://doi.org/10.1016/j.tplants.2017.09.003

Schmid, R., Heuckeroth, S., Korf, A., Smirnov, A., Myers, O., Dyrlund, T.S., Bushuiev, R., Murray, K.J., Hoffmann, N., Lu, M., Sarvepalli, A., Zhang, Z., Fleischauer, M., Dührkop, K., Wesner, M., Hoogstra, S.J., Rudt, E., Mokshyna, O., Brungs, C., Ponomarov, K., Mutabdžija, L., Damiani, T., Pudney, C.J., Earll, M., Helmer, P.O., Fallon, T.R., Schulze, T., Rivas-Ubach, A., Bilbao, A., Richter, H., Nothias, L.-F., Wang, M., Orešič, M., Weng, J.-K., Böcker, S., Jeibmann, A., Hayen, H., Karst, U., Dorrestein, P.C., Petras, D., Du, X., Pluskal, T., 2023. Integrative analysis of multimodal mass spectrometry data in MZmine 3. Nat. Biotechnol. 41, 447–449. https://doi.org/10.1038/s41587-023-01690-2

Schymanski, E.L., Jeon, J., Gulde, R., Fenner, K., Ruff, M., Singer, H.P., Hollender, J., 2014. Identifying Small Molecules via High Resolution Mass Spectrometry: Communicating Confidence. Environ. Sci. Technol. 48, 2097–2098. https://doi.org/10.1021/es5002105

Shannon, P., Markiel, A., Ozier, O., Baliga, N.S., Wang, J.T., Ramage, D., Amin, N., Schwikowski, B., Ideker, T., 2003. Cytoscape: A Software Environment for Integrated Models of Biomolecular Interaction Networks. Genome Res. 13, 2498–2504. https://doi.org/10.1101/gr.1239303

Shavrukov, Y., 2013. Salt stress or salt shock: which genes are we studying? J. Exp. Bot. 64, 119–127. https://doi.org/10.1093/jxb/ers316

Si, C.-L., Kim, J.-K., Bae, Y.-S., Li, S.-M., 2009. Phenolic Compounds in the Leaves of *Populus ussuriensis* and their Antioxidant Activities. Planta Med. 75, 1165–1167. https://doi.org/10.1055/s-0029-1185476

Singh, A., 2021. Soil salinization management for sustainable development: A review. J. Environ. Manage. 277, 111383. https://doi.org/10.1016/j.jenvman.2020.111383

Skerrett, M., Tyerman, S.D., 1994. A channel that allows inwardly directed fluxes of anions in protoplasts derived from wheat roots. Planta 192, 295–305. https://doi.org/10.1007/BF00198563

Slama, I., Abdelly, C., Bouchereau, A., Flowers, T., Savouré, A., 2015. Diversity, distribution and roles of osmoprotective compounds accumulated in halophytes under abiotic stress. Ann. Bot. 115, 433–447. https://doi.org/10.1093/aob/mcu239

Sonar, P., Bellucci, L., Mossa, A., Heidarsson, P.O., Kragelund, B.B., Cecconi, C., 2020. Effects of Ligand Binding on the Energy Landscape of Acyl-CoA-Binding Protein. Biophys. J. 119, 1821–1832. https://doi.org/10.1016/j.bpj.2020.09.016

Sonmez, S., Buyuktas, D., Okturen, F., Citak, S., 2008. Assessment of different soil to water ratios (1:1, 1:2.5, 1:5) in soil salinity studies. Geoderma, Antarctic Soils and Soil Forming Processes in a Changing Environment 144, 361–369. https://doi.org/10.1016/j.geoderma.2007.12.005

Steppuhn, H., Kort, J., Wall, K.G., 2008. First year growth response of selected hybrid poplar cuttings to root-zone salinity. Can. J. Plant Sci. 88, 473–483. https://doi.org/10.4141/CJPS07098

Sui, D., Wang, B., 2020. Transcriptome Analysis Reveals Complex Defensive Mechanisms in Salt-Tolerant and Salt-Sensitive Shrub Willow Genotypes under Salinity Stress. Int. J. Genomics 2020, e6870157. https://doi.org/10.1155/2020/6870157

Sumner, L.W., Amberg, A., Barrett, D., Beale, M.H., Beger, R., Daykin, C.A., Fan, T.W.-M., Fiehn, O., Goodacre, R., Griffin, J.L., Hankemeier, T., Hardy, N., Harnly, J., Higashi, R., Kopka, J., Lane, A.N., Lindon, J.C., Marriott, P., Nicholls, A.W., Reily, M.D., Thaden, J.J., Viant, M.R., 2007. Proposed minimum reporting standards for chemical analysis. Metabolomics 3, 211–221. https://doi.org/10.1007/s11306-007-0082-2

Tarchoune, I., Degl'Innocenti, E., Kaddour, R., Guidi, L., Lachaâl, M., Navari-Izzo, F., Ouerghi, Z., 2012. Effects of NaCl or Na2SO4 salinity on plant growth, ion content and photosynthetic activity in Ocimum basilicum L. Acta Physiol. Plant. 34, 607–615. https://doi.org/10.1007/s11738-011-0861-2

Teakle, N.L., Tyerman, S.D., 2010. Q-Mechanisms of Cl- transport contributing to salt tolerance. Plant Cell Environ. 33, 566–589. https://doi.org/10.1111/j.1365-3040.2009.02060.x

Tyśkiewicz, K., Konkol, M., Kowalski, R., Rój, E., Warmiński, K., Krzyżaniak, M., Gil, Ł., Stolarski, M.J., 2019. Characterization of bioactive compounds in the biomass of black locust, poplar and willow. Trees 33, 1235–1263. https://doi.org/10.1007/s00468-019-01837-2

van Zelm, E., Zhang, Y., Testerink, C., 2020. Q-Salt tolerance mechanisms of plants. Annu. Rev. Plant Biol. 71, 403–433. https://doi.org/10.1146/annurev-arplant-050718-100005

Volf, M., Hrcek, J., Julkunen-Tiitto, R., Novotny, V., 2015. To each its own: differential response of specialist and generalist herbivores to plant defence in willows. J. Anim. Ecol. 84, 1123–1132. https://doi.org/10.1111/1365-2656.12349

Volf, M., Volfová, T., Hörandl, E., Wagner, N.D., Luntamo, N., Salminen, J.-P., Sedio, B.E., 2022. Abiotic stress rather than biotic interactions drives contrasting trends in chemical richness and variation in alpine willows. Funct. Ecol. 36, 2701–2712. https://doi.org/10.1111/1365-2435.14169

Volk, T.A., Abrahamson, L.P., Nowak, C.A., Smart, L.B., Tharakan, P.J., White, E.H., 2006. The development of short-rotation willow in the northeastern United States for bioenergy and bioproducts, agroforestry and phytoremediation. Biomass Bioenergy, Proceedings of the 5th Biennial meeting of the Short Rotation Woody Crops Operations Working Group in conjunction with International Energy Agency Bioenergy, Task 30, Short Rotation Crops for Bioenergy Systems and International Union of Forest Research Organization, Working Unit 1.09.01, Integrated Research in Temperate Short-Rotation Energy Plantations 30, 715–727. https://doi.org/10.1016/j.biombioe.2006.03.001

Watanabe, M., Hoefgen, R., 2019. Sulphur systems biology—making sense of omics data. J. Exp. Bot. 70, 4155–4170. https://doi.org/10.1093/jxb/erz260

Watanabe, S., Kojima, K., Ide, Y., Sasaki, S., 2000. Effects of saline and osmotic stress on proline and sugar accumulation in Populus euphratica in vitro. Plant Cell Tissue Organ Cult. 63, 199–206. https://doi.org/10.1023/A:1010619503680

Wege, S., Gilliham, M., Henderson, S.W., 2017. Chloride: not simply a 'cheap osmoticum', but a beneficial plant macronutrient. J. Exp. Bot. 68, 3057–3069. https://doi.org/10.1093/jxb/erx050

Wei, H., Movahedi, A., Xu, C., Sun, W., Li, L., Wang, P., Li, D., Zhuge, Q., 2020. Overexpression of PtHMGR enhances drought and salt tolerance of poplar. Ann. Bot. 125, 785–803. https://doi.org/10.1093/aob/mcz158

White, P.J., Broadley, M.R., 2001. Chloride in Soils and its Uptake and Movement within the Plant: A Review. Ann. Bot. 88, 967–988. https://doi.org/10.1006/anbo.2001.1540

Wu, D., Cai, S., Chen, M., Ye, L., Chen, Z., Zhang, H., Dai, F., Wu, F., Zhang, G., 2013. Tissue Metabolic Responses to Salt Stress in Wild and Cultivated Barley. PLOS ONE 8, e55431. https://doi.org/10.1371/journal.pone.0055431

Xia, L., Xiaodong, M., Yunhe, C., Junxiang, L., Junzhu, Z., Feifei, Z., Zhenyuan, S., Lei, H., 2021. Transcriptomic and metabolomic insights into the adaptive response of Salix viminalis to phenanthrene. Chemosphere 262, 127573. https://doi.org/10.1016/j.chemosphere.2020.127573

Xiao, J., Muzashvili, T.S., Georgiev, M.I., 2014. Advances in the biotechnological glycosylation of valuable flavonoids. Biotechnol. Adv. 32, 1145–1156. https://doi.org/10.1016/j.biotechadv.2014.04.006

Yancey, P.H., 2005. Organic osmolytes as compatible, metabolic and counteracting cytoprotectants in high osmolarity and other stresses. J. Exp. Biol. 208, 2819–2830. https://doi.org/10.1242/jeb.01730

Yang, Y., Guo, Y., 2018. Q-Elucidating the molecular mechanisms mediating plant salt-stress responses. New Phytol. 217, 523–539. https://doi.org/10.1111/nph.14920

Zhang, Y., Fang, J., Wu, X., Dong, L., 2018. Na+/K+ Balance and Transport Regulatory Mechanisms in Weedy and Cultivated Rice (Oryza sativa L.) Under Salt Stress. BMC Plant Biol. 18, 375. https://doi.org/10.1186/s12870-018-1586-9

Zhou, J., Guo, J., Chen, Q., Wang, B., He, X., Zhuge, Q., Wang, P., 2022. Different color regulation mechanism in willow barks determined using integrated metabolomics and transcriptomics analyses. BMC Plant Biol. 22, 530. https://doi.org/10.1186/s12870-022-03909-x

Zhou, J., Huang, J., Tian, X., Zheng, J., He, X., 2020. Transcriptome analysis reveals dynamic changes in the salt stress response in Salix. J. For. Res. 31, 1851–1862. https://doi.org/10.1007/s11676-019-00941-w

Zhou, Z., Luo, M., Zhang, H., Yin, Y., Cai, Y., Zhu, Z.-J., 2022. Metabolite annotation from knowns to unknowns through knowledge-guided multi-layer metabolic networking. Nat. Commun. 13, 6656. https://doi.org/10.1038/s41467-022-34537-6

Zörb, C., Geilfus, C.-M., Dietz, K.-J., 2019. Salinity and crop yield. Plant Biol. 21, 31–38. https://doi.org/10.1111/plb.12884

Zou, Y., Zhang, Y., Testerink, C., 2022. Q-Root dynamic growth strategies in response to salinity. Plant Cell Environ. 45, 695–704. https://doi.org/10.1111/pce.14205

1081

1082

11 FIGURES

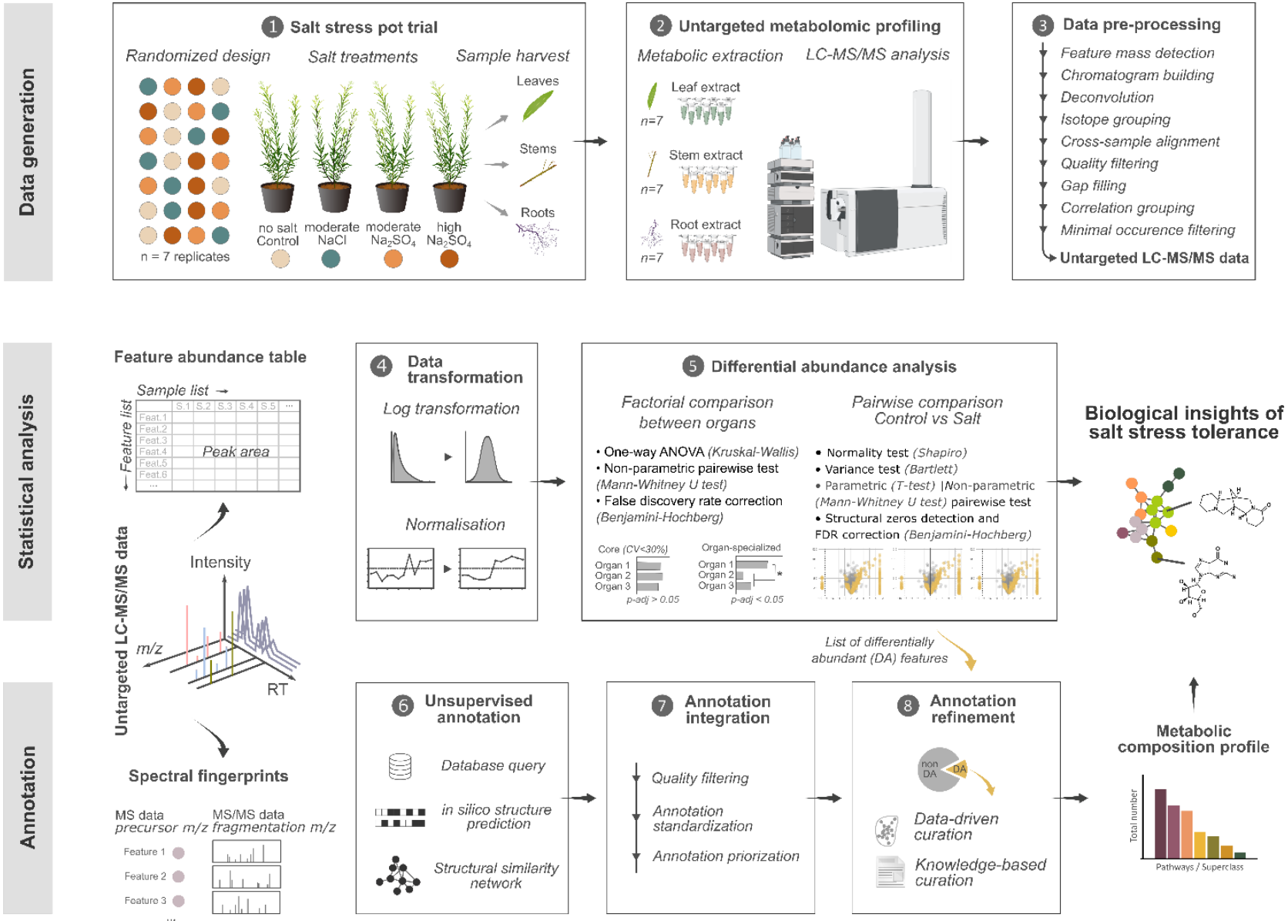

***Figure 1**: Workflow for untargeted metabolomics approach.*

A randomized pot trial treated willows with salt solutions or water controls (7 replicates per treatment) to explore variation in anion-specific salt tolerance mechanisms across organs. Metabolites were extracted from root, stem and leaf samples and analysed by LC-MS/MS. Resulting chromatographic data were pre-processed using MZmine for features mass detection, cross-sample alignment and quality filters. Statistical analysis used a cross-sample aligned peak area table. After log transformation and Eigen MS normalization, univariate analysis was used to factorially compare feature peak areas across willow organs in controls, while pairwise comparisons were used to identify differentially abundant (DA) compounds between each salt treatment compared to controls. Parametric or non-parametric tests were used based on feature peak area normality and variance homogeneity, finally a false discovery rate correction was applied to account for multiple testing. Annotation strategy used precursors information and corresponding spectral fingerprints (when available) to query multiple databases and for *in silico* structure prediction to generate a list of annotation candidates (unsupervised annotation). After standardizing compounds identity information and assigning prioritization criteria, the best candidate was retained. Annotation was further refined for compounds identified as differentially abundant due to salt treatment and used data-driven (structural similarity networking) and knowledge-driven (literature) curation.

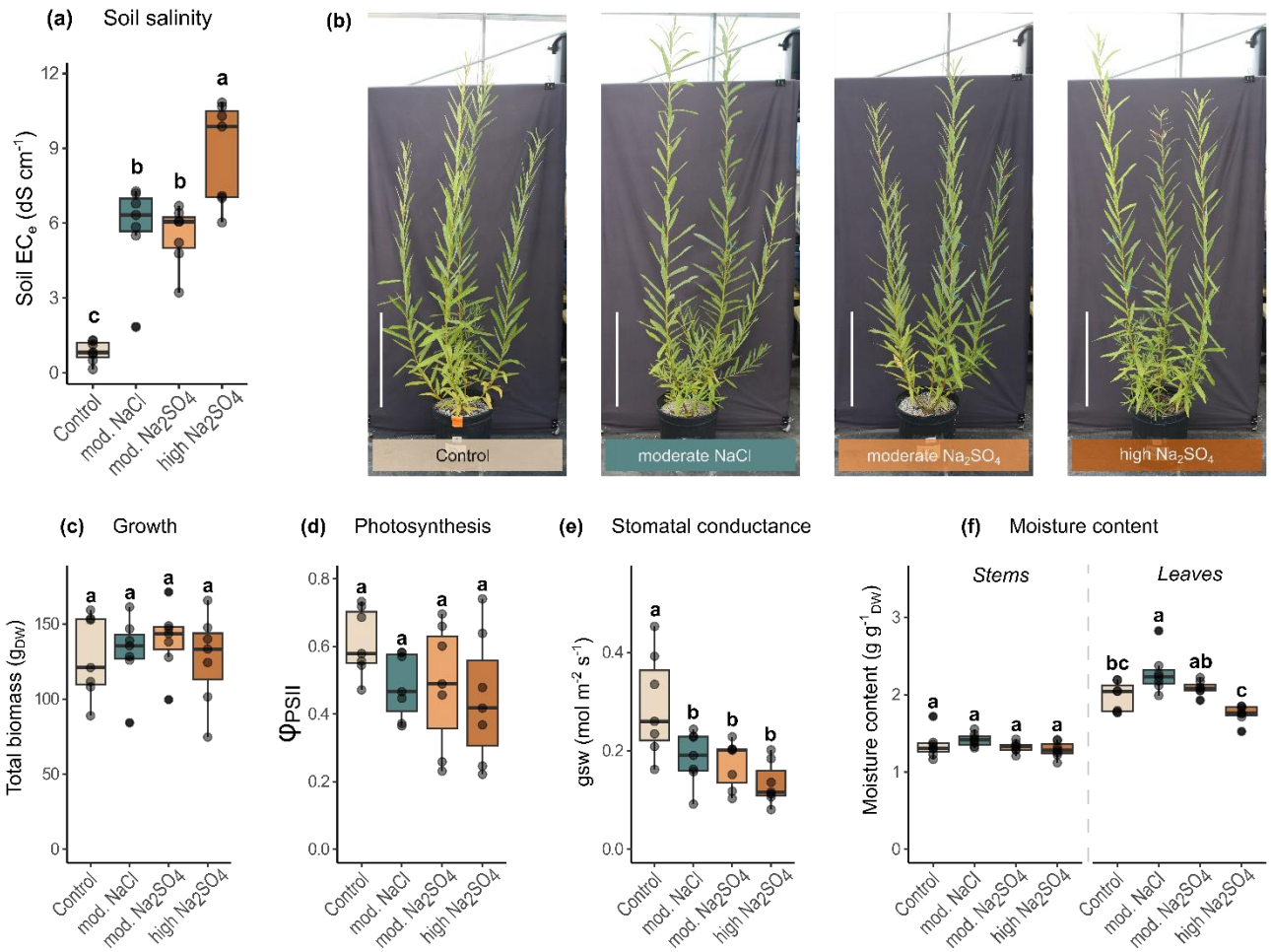

Figure 2: Physiological assessment of salt stress on Salix miyabeana 'SX64'.

(a) Following 56 days of root establishment, salinity in planted pots was progressively built-up over 28 days to reach the final saturated soil electroconductivity (EC), as inferred from a (1:1) soil-to-water extract. **(b)** Representative willow photographs, on harvest day, in response to salt treatments (white scale bars: 50 cm). The impact of moderate NaCl, moderate Na_2SO_4 and high Na_2SO_4 were quantified on **(c)** total biomass (dry weight), **(d)** photosystem II efficiency evaluated using the LI-COR 600 parameter phiPSII, **(e)** stomatal conductance gsw, **(f)** stems and leaves moisture contents. Boxes represent median and quartiles while whiskers extend to the largest value within 1.5 times the inter-quartile range (IQR) from the hinge. Dots represent individual plants (n=7). Significant differences ($p<0.05$) indicated by letters were determined by two-way ANOVA followed by Tukey's post hoc test.

1095

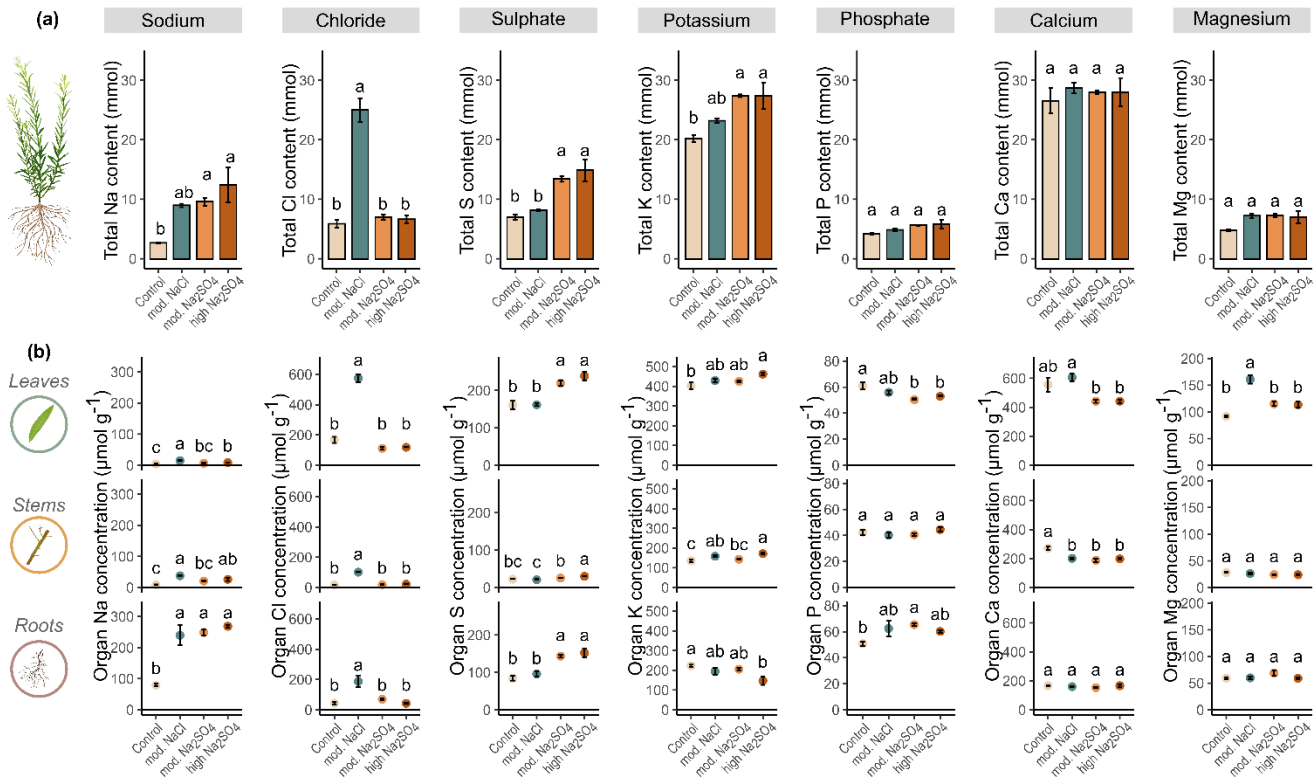

Figure 3: Elemental analysis of mineral nutrients.

Elemental analyses include sodium (Na), chloride (Cl), sulphur (S), potassium (K), phosphorus (P), calcium (Ca), and magnesium (Mg). **(a)** Total element content (mmol) combined from the leaves, stems and roots presented. The bars indicate mean values within each organ ± standard error (n=3). **(b)** Element concentration within a single organ (µmol g_{DW}^{-1}) is shown. The dots represent mean values ± standard error (n=3). Letters indicate significant differences ($p<0.05$) between control, moderate NaCl, moderate Na_2SO_4, and high Na_2SO_4 treatments and were determined using two-way ANOVA followed by Tukey's post hoc test. Mineral elements ratios (K^+/Na^+; Ca^{2+}/Na^+; K^+/Ca^{2+}) are presented in Supplementary – Fig.S4.

1096

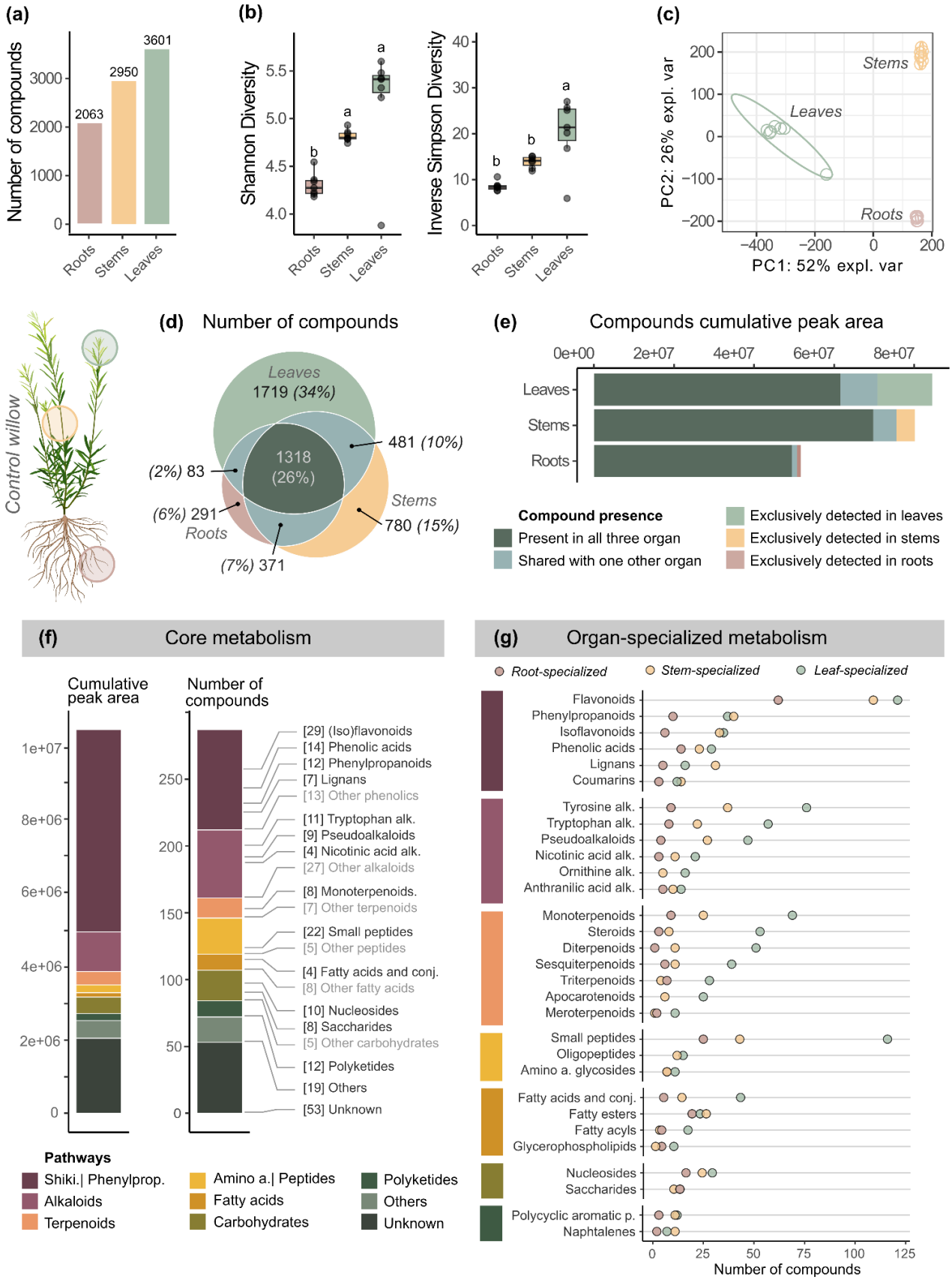

Figure 4: Willow metabolic composition.

Organs (leaves, stems and roots) were separately collected from control willows and analysed for metabolomic profiling. **(a)** Total number of consistently detected metabolites within each major organ (present in at least 4

replicates out of 7). **(b)** Comparison of organ metabolic richness using Shannon and Inverse Simpson diversity indices (n=7), different letters indicate significant differences (ANOVA, Tukey HSD, $p<0.05$). **(c)** Principal component analysis depicting dissimilarity in organ composition based on Bray-Curtis distances, ellipses are for standard deviation. **(d)** Venn diagram illustrating the distribution of metabolites across organs as unique to one or shared between multiple. **(e)** Cumulative peak areas of metabolites present in each organ, categorised based on their exclusive presence in the respective organ or shared across multiple organs. **(f)** Cumulative peak area and number of core metabolites (compounds present across the entire plant, with no significant variation of abundance between organs) classified per metabolic pathways, with composition details of main superclasses. **(g)** Count of compounds significantly higher in one organ compared to the other two (ANOVA, Tukey HSD, $p<0.05$), revealing dominant organ-specialisation of some metabolic superclasses.

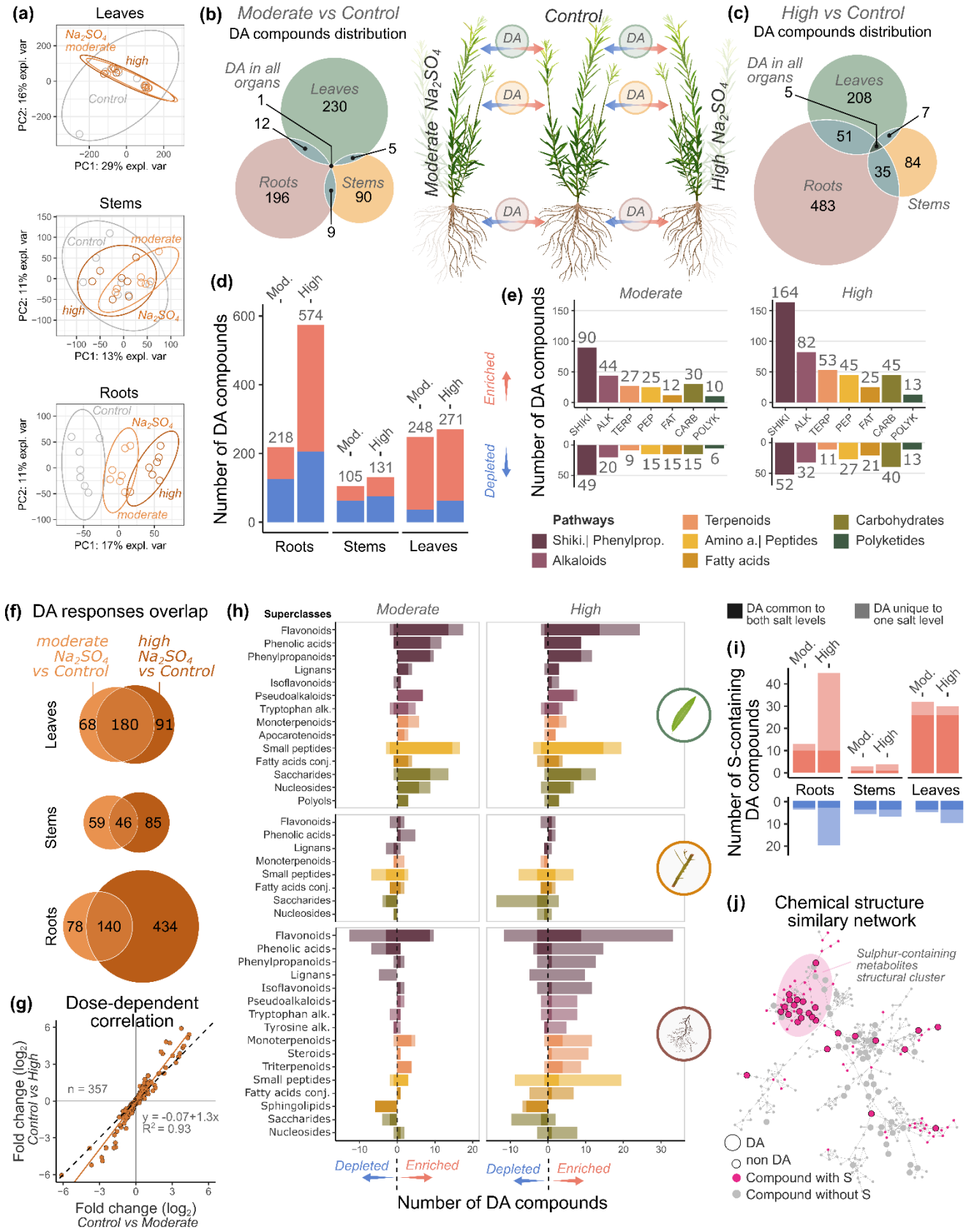

Figure 5: Willow metabolic response to sodium sulphate (Na_2SO_4) salt and its variation with dose

(a) Principal component analysis (PCA) based on Bray-Curtis distance, illustrating metabolic profile dissimilarity between control, moderate Na_2SO_4 and high Na_2SO_4 at organ scale (n=7), including standard deviation ellipse

(95% confidence interval). **(b)** Organ distribution of differentially abundant (DA) compounds between control and moderate concentration Na_2SO_4-treated willows ($p<0.05$). **(c)** Organ distribution of differentially abundant compounds between control and high concentration Na_2SO_4-treated willows ($p<0.05$). **(d)** Overview of significantly enriched and depleted compounds across organs, comparing DA of control against moderate Na_2SO_4 and control against high Na_2SO_4. **(e)** Distribution of enriched and depleted DA compounds across metabolic pathways for moderate and high Na_2SO_4 treatments compared to controls. **(f)** Metabolic response overlap across both Na_2SO_4 concentrations, representing the number of DA compounds common and unique to a single dose DA, at organ scale. **(g)** Dose-dependent correlation of compounds consistently DA across Na_2SO_4 levels within the same organ (excluding salt-induced/salt-suppressed compounds with infinite fold change), representing the fold change (log2) of average peak areas (n=7) under moderate Na_2SO_4 relative to control against high Na_2SO_4 relative to control. **(h)** Sub-selection of main superclasses altered by moderate or high concentration of Na_2SO_4 compared to controls, illustrating enriched and depleted compounds distribution at organ scale. DA compounds shared between both treatment levels are highlighted by the darker section of the bars. **(i)** Distribution of enriched and depleted sulphur-containing DA compounds at organ scale, comparing both levels of Na_2SO_4. Shared compounds are highlighted by the darker section of the bars. **(j)** Molecular network of compounds MS/MS spectra similarities (cosine>0.6) computed in the GNPS environment and visualised in Cytoscape. Dots are color-coded based on the presence of sulphur (pink represents S-containing compounds) and dot size highlights significantly different compounds (larger dots are DA compounds). A major cluster containing 16 S-containing and structurally similar DA compounds is circled by an ellipse.

1098

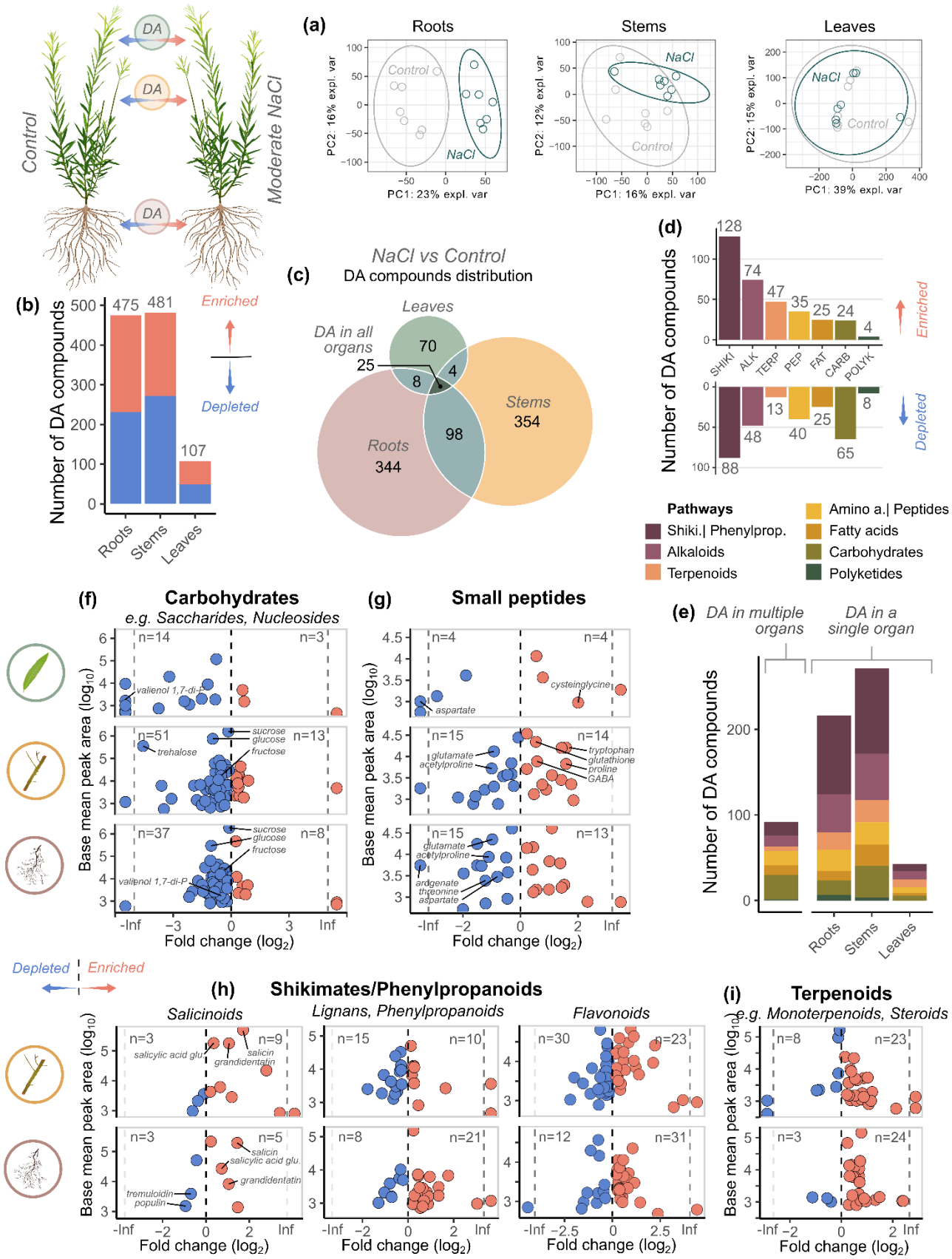

Figure 6: Willow metabolic response to sodium chloride (NaCl) salt.

(a) Principal component analysis (PCA) based on Bray-Curtis distance, illustrating metabolic profile dissimilarity between control and moderate NaCl at organ scale (n=7), including standard deviation ellipse (95% confidence

interval) **(b)** Overview of significantly enriched and depleted compounds across organs. **(c)** Organ distribution of differentially abundant (DA) compounds between control and moderate concentration NaCl-treated willows ($p<0.05$). **(d)** Distribution of enriched and depleted DA compounds across metabolic pathways. **(e)** Metabolic profile at pathway level of DA compounds shared between multiple organs and unique to roots, stems or leaves. Sub-selection of main pathways or superclasses altered by moderate NaCl compared to controls, illustrating enriched and depleted compounds distribution at organ scale for **(f)** carbohydrates, including saccharides and nucleosides, **(g)** small peptides, **(h)** and 3 major superclass of shikimates and phenylpropanoids pathway: salicinoids, lignans, phenylpropanoids, flavonoids, as well as **(i)** terpenoids, including monoterpenoids and steroids. Dots are color-coded by regulation (blue: depleted, red: enriched by salt treatment compared to control). Base mean area reflects average peak area across all compared samples.

1099

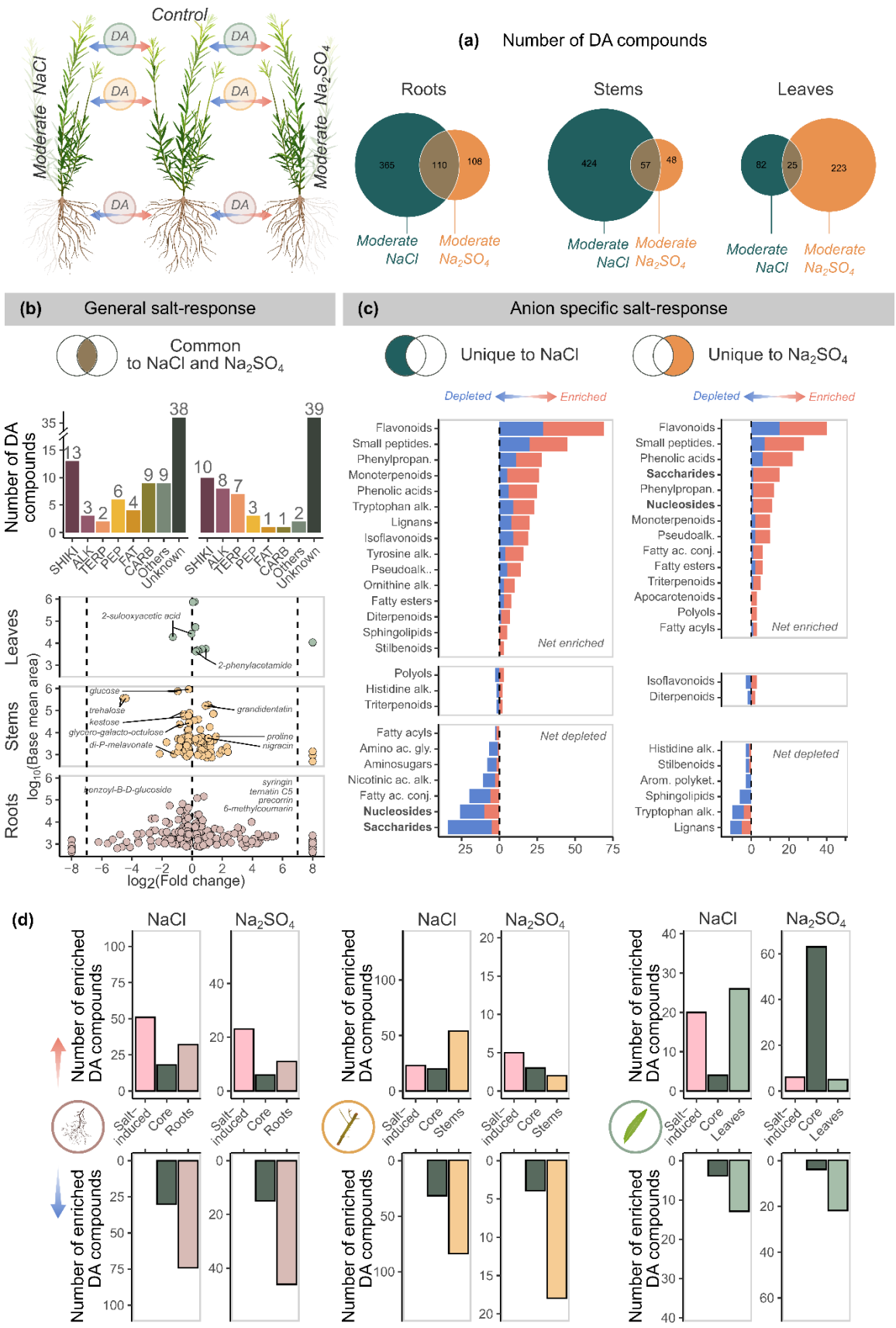

Figure 7: General willow salt response and anion specific tailored responses.

(a) Venn diagrams showing DA metabolic responses overlap in roots, stems, and leaves under moderate NaCl and Na_2SO_4 stress. **(b**) Pathway profile of commonly enriched and depleted compounds in response to moderate salt stress. Fold change graph illustrated enriched and depleted compounds distribution at organ scale. **(c)** Superclass profiles of NaCl- and Na_2SO_4-specific responses, ordered as net enriched, equal, and net depleted, with differential pattering of nucleosides and saccharides highlighted in bold. **(d)** Metabolic response to moderate NaCl and moderate Na_2SO_4 categorised based on compounds distribution across the whole plant: salt-induced compounds (not detected in controls), core compounds (present in all organs at stable state in controls), organ-specialised compounds: roots, stems or leaves (present in a higher abundance in a specific organ, based on controls). Bar graphs are split as depleted and enriched compounds to highlight patterning of the DA compounds.

1102